THERMAL-ELECTRICAL MODELLING OF ELECTRICAL DISCHARGE MACHINING PROCESS

A THESIS SUBMITTED IN PARTIAL FULFILMENT
OF THE REQUIREMENTS FOR THE DEGREE OF

Master of Technology

in

Mechanical Engineering

By

SASMEETA TRIPATHY

Department of Mechanical Engineering

National Institute of Technology

Rourkela

2007

THERMAL-ELECTRICAL MODELLING OF ELECTRICAL DISCHARGE MACHINING PROCESS

A THESIS SUBMITTED IN PARTIAL FULFILMENT
OF THE REQUIREMENTS FOR THE DEGREE OF

Master of Technology

in

Mechanical Engineering

By

SASMEETA TRIPATHY

Under the Guidance of

Prof. C.K.BISWAS

Department of Mechanical Engineering

National Institute of Technology

Rourkela

2007

National Institute of Technology
Rourkela

CERTIFICATE

This is to certify that thesis entitled, "THERMAL-ELECTRICAL MODELLING OF ELECTRICAL DISCHARGE MACHINING PROCESS**"** submitted by Ms. SASMEETA TRIPATHY in partial fulfillment of the requirements for the award of Master of Technology Degree in Mechanical Engineering with specialization in "Production Engineering" at National Institute of Technology, Rourkela (Deemed University) is an authentic work carried out by her under my supervision and guidance.

To the best of my knowledge, the matter embodied in this thesis has not been submitted to any other university/ institute for award of any Degree or Diploma.

Date:

Prof. C.K.BISWAS
Dept. of Mechanical Engineering
National Institute of Technology
Rourkela-769008

ACKNOWLEDGEMENT

It is with a feeling of great pleasure that I would like to express my most sincere heartfelt gratitude to Prof.C.K.Biswas, Asst. Professor, Dept. of Mechanical Engineering, NIT, Rourkela for suggesting the topic for my thesis report and for his ready and able guidance through out the course of my preparing the report. I am greatly indebted to him for his constructive suggestions and criticism from time to time during the course of progress of my work.

I express my sincere thanks to Prof. B.K.Nanda, Head of the Department of Mechanical Engineering, NIT, Rourkela for providing me the necessary facilities in the department.

I express my sincere gratitude to Prof. K.P.Maity, Co-ordinator of M.E. course for his timely help during the course of work.

I am also thankful to all the staff members of the department of Mechanical Engineering and to all my well wishers for their inspiration and help.

I feel pleased and privileged to fulfill my parents ambition and I am greatly indebted to them for bearing the inconvenience during my M.E. course.

Date:

Sasmeeta Tripathy

Roll No.:-20503051

LIST OF FIGURES

LIST OF TABLES

ABSTRACT

Non-traditional machining has grown out of the need to machine exotic engineering metallic materials, composite materials and high tech ceramics having good mechanical properties and thermal characteristics as well as sufficient electrical conductivity. Electric Discharge machinery developed in late 1940's has been accepted worldwide as a standard process in manufacturing and is capable of machining geometrically complex or hard material components, that are precise and difficult-to-machine such as heat treated tool steels, composites, super alloys, ceramics, hastalloys, nitralloy, nemonics, carbides, heat resistant steels etc. being widely used in die and mold making industries, aerospace, aeronautics and nuclear industries

The thermal erosion theory is the most accepted mathematical model for evaluating material removal from electrodes during EDM process. It postulates that the process involves melted electrode and its evaporation by the discharge energy dissipated on electrode surface. Part of the melted and evaporated material is then ejected from electrode by force of different natures.

Keeping this in view, the present work has been undertaken to generate a thermal-electrical model for sparks generated by electrical discharge in a liquid media and to determine the temperature distribution of tool and work piece. For a single discharge test, copper and En-19 was used as specimens. The amount of heat dissipated varies with the thermal-physical properties of the conductor. The model is developed by using ANSYS software. ANSYS uses the finite-element method to solve the underlying governing equations and the associated problem-specific boundary conditions. Material Removal Rate, Surface Roughness and the maximum temperature reached in the discharge channel is determined.

CONTENTS

CHAPTER – 1

1.1 BACKGROUND

The new concept of manufacturing uses non-conventional energy sources like sound, light, mechanical, chemical, electrical, electrons and ions. With the industrial and technological growth, development of harder and difficult to machine materials, which find wide application in aerospace, nuclear engineering and other industries owing to their high strength to weight ratio, hardness and heat resistance qualities has been witnessed. New developments in the field of material science have led to new engineering metallic materials, composite materials and high tech ceramics having good mechanical properties and thermal characteristics as well as sufficient electrical conductivity so that they can readily be machined by spark erosion. Non-traditional machining has grown out of the need to machine these exotic materials. The machining processes are non-traditional in the sense that they do not employ traditional tools for metal removal and instead they directly use other forms of energy. The problems of high complexity in shape, size and higher demand for product accuracy and surface finish can be solved through non-traditional methods. Currently, non-traditional processes possess virtually unlimited capabilities except for volumetric material removal rates, for which great advances have been made in the past few years to increase the material removal rates. As removal rate increases, the cost effectiveness of operations also increase, stimulating ever greater uses of non traditional process. The Electrical Discharge Machining process is employed widely for making tools, dies and other precision parts [1].

Electrical Discharge machining (EDM) has been replacing drilling, milling, grinding and other traditional machining operations and is now a well established machining option in many manufacturing industries throughout the world. Modern Electric Discharge machinery developed in late 1940's has been accepted worldwide as a standard process in manufacturing and is capable of machining geometrically complex or hard material components, that are precise and difficult-to-machine such as heat treated tool steels, composites, super alloys, ceramics, hastalloys, nitralloy, nemonics, carbides, heat resistant steels etc. being widely used in die and mold making industries, aerospace, aeronautics and nuclear industries. Electric

Discharge Machining has also made its presence felt in the new fields such as sports, medical and surgical, instruments, optical, including automotive R&D areas [2, 3].

1.2 PRINCIPLE OF EDM:

In principle, EDM process is thermo-electric in nature and removes material from the work piece by series of discrete sparks between tool and work electrodes immersed in a dielectric medium. The electrode is moved towards the work piece until the gap is small enough to ionize the dielectric. Short duration discharges are generated in a liquid dielectric gap, which separates tool and work piece. The dielectric fluid makes it possible to flush eroded particles (mainly in form of hollow spheres) from the gap and it is really important to maintain this flushing continuously.

The material is removed with the erosive effect of the electrical discharges from tool and work piece. There is no direct contact between electrode and work piece which eliminate mechanical stresses, chatter and vibration problems during machining [4]. Since erosion is produced by electrical discharges, both electrode and work piece have to be electrically conductive. In this process, the machining force is much smaller than that in cutting processes, because molten metal can be removed with a very small force. EDM uses electric energy by discharge which occurs as a result of dielectric breakdown between positive tool electrode and negative work piece. As tool electrode approaches to a work piece, the electric filed between tool and work piece is larger and larger. And then it comes to a point where a spark occurs. This is known as the fluid-ionization point and it is based on the dielectric strength of the fluid and the distance between the electrode and work piece. Dielectric fluid has non conductive property which is between anode and cathode. When discharge occurs, the voltage drops about to the range of from 25V to 45V. Figure 1.1 illustrates the graph of variation of current according to voltage. The area which is used in electric discharge machining b-c is the spark discharge area, and d-e is the arc discharge area. When spark discharge occurs, which is the electricity flowing through the ionized column of dielectric, there is no variation of voltage but the amplitude of current rises quickly to a constant value set by operator. Within the ionized column, electrons separate from the dielectric-fluid atoms and flow from the negative-polarity electrode toward the positive-polarity work piece. Since the dielectric-fluid atoms in the column are missing electrons,

they are positively charged, and flow from the positive polarity work piece toward negative-polarity electrode. This streaming of electrons and positive ions is known as plasma channel. Plasma channels that are surrounded by bubbles which occur by vaporization of dielectric fluid grow during on-time [5].

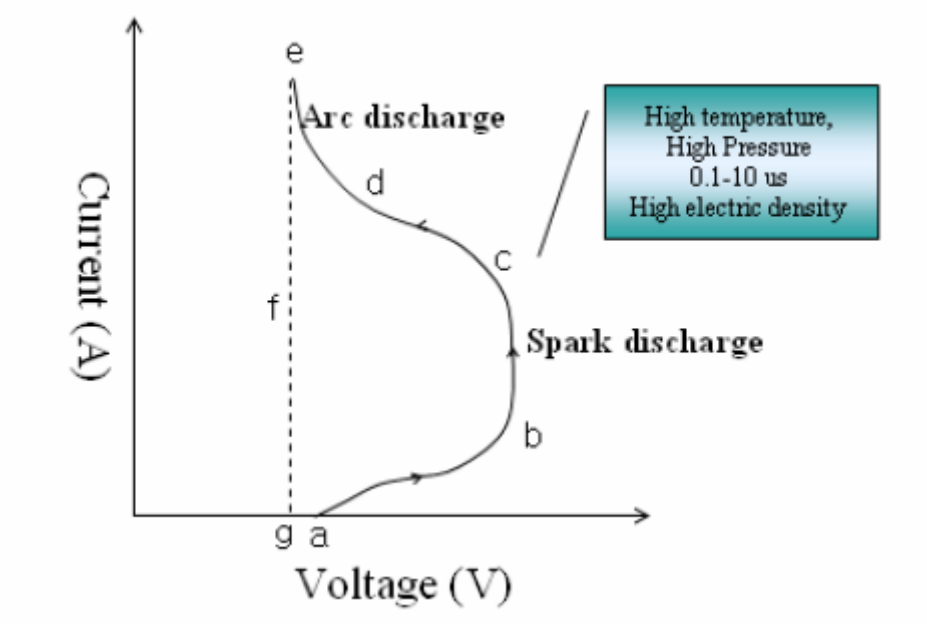

Fig.1.1 Graph for current variation with voltage

1.3 Four successive steps by which an electrical discharge between the tool electrode and the work piece proceeds [6]:

1. The ignition phase
2. Formation of the plasma channel
3. Melting and evaporation of a small amount of work piece material
4. Ejection of the liquid molten material

1.3.1 The ignition phase

An electrical tension is applied between electrode and work piece, creating an electrical field, characterized by the voltage gradient, expressed by the ratio of tension to distance, as well

as some other items (roughness profile of tool and work piece, debris in the gap,). At the places where the gradient is maximal (usually at the highest points on the surface), electrons are emitted by the cathode (Fig1.2 (a)).These electrons are called the primary electrons. The primary electrons are attracted by the anode and start moving towards it. On their way through the dielectric, the primary electrons collide with metal atoms of the dielectric. As a consequence, these dielectric atoms split up in positive ions and electrons. These are called the secondary electrons (Fig. 1.2 (b)).

1.3.2 Formation of the plasma channel

The positive ions originating from the dielectric are attracted towards the cathode. When they hit the cathode, they free some more electrons. This process is called the secondary emission. These electrons also move towards the anode and split up some more neutral dielectric atoms. The current, created by both the electrons and the ions increases drastically and the dielectric starts heating locally. This decreases the electrical resistance and the current increases further. The dielectric continues heating and vapor and even a plasma channel are created (Fig 1.2(b).). The plasma channel is characterized by high pressure and temperature. The formation of the plasma channel is also called the voltage breakdown because when the plasma channel is created, the voltage drops from the higher, user specified open circuit tension to the breakdown voltage which is determined by the material combination of electrode and work piece (for the copper-steel combination it is from 20 to 25V). In normal cases, the voltage breakdown is initiated when the value of the electrical field reaches about 10^4V/mm. The time which elapses between applying the voltage and the voltage and the breakdown (and thus also the beginning of the discharge) is called the ignition delay time. During machining, debris particles (the chips) caused by machining and decomposition of the dielectric due to the high temperatures, are present in the dielectric fluid. Furthermore, powder particles can be added on purpose to the dielectric. In these cases, the particles in the dielectric form discharge paths which increase the voltage gradient. Consequently, the discharge takes place more easily and the gap is increased.

1.3.3 Melting and evaporation

The plasma channel is maintained by the EDM machine for a user specified time. During this time, the anode and cathode surfaces are bombarded by electrons and ions respectively.

When an electron or an ion collides with the surface, its kinetic energy is transformed into heat (Fig1.2(c)). This heat induces melting and a partial evaporation of the surface. The amount of molten material depends among other things from the number of electrons or ions that collide with the surface. The number of colliding particles per discharge depends on the current of the discharge and the discharge time. There is an important difference in mass between electrons and ions. Metal ions are much heavier than electrons and so their kinetic energy is much higher. However, due to the higher inertia of ions, it takes more time to bring them to a certain speed. Therefore, when short discharge times are applied, especially the electrons cause a high heat while only a limited amount of ions collide with the cathode. The speed of the ions is still low, so they need time to travel over a certain distance. It is only when longer discharge times are used that many ions can reach the surface of the cathode at a high speed. The high kinetic energy of the ions generates a lot of heat, melting the cathode surface.

1.3.4 Ejection of the liquid molten material

At the end of the user specified discharge time, the EDM machine stops the current abruptly. As a consequence, the plasma channel collapses and so the pressure on the molten cathode and anode surface (caused by the plasma channel) drops suddenly. This makes the molten materials at both electrode and work piece to boil violently and small droplets of liquid metal are ejected from the molten metal pool (Fig1.2 (d)). The removed material is evacuated by the flow of the dielectric fluid. This is the main material removal process in EDM. The main part is removed by the sudden and intense boiling at the end of the discharge.

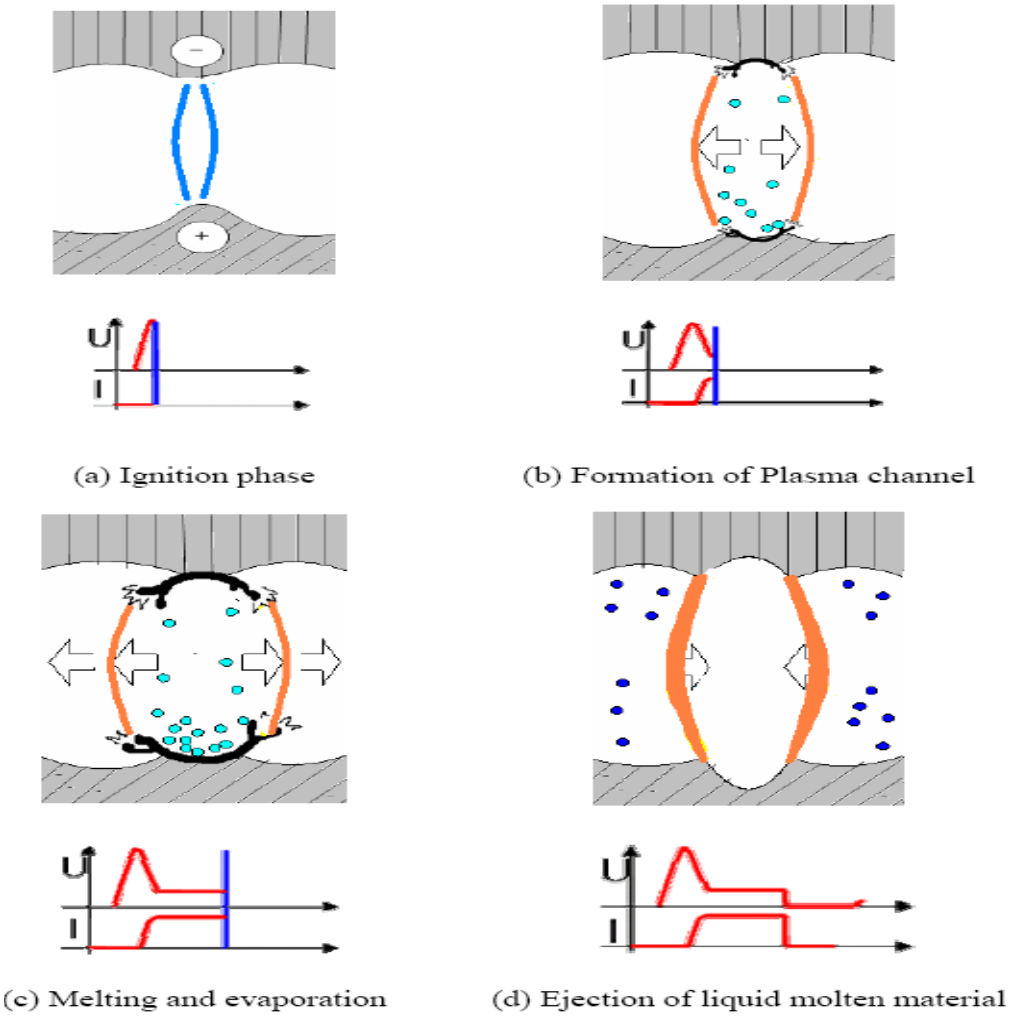

Fig.1.2 (a-d) Successive Stages of EDM Process

1.4 CLASSIFICATION OF EDM PROCESS:

Basically, there are two different types of EDM as shown in Fig.1.3 (a) and 1.3(b):

(a) Die-sinking EDM

(b) Wire-cut EDM

1.4.1 Die-sinking EDM:

It reproduces the shape of the tool used (electrode) in the part where the tool shape complements the final desired shape of the work piece. The wear has to be very low, in order to

keep the electrode original shape unmodified during the whole machining process. The asymmetry in the material removal rate is thus crucial for die-sinking. The electrode is generally of copper or graphite, and the dielectric is oil. In case of die-sinking EDM the tool is usually the anode and the workpiece is the cathode for coarse machining operations while the polarities are reversed for fine machining operations. During any single discharge the anode starts to melt first because it absorbs the fast moving electrons at the start of the pulse but re-solidifies fast because of the expanding radius of the plasma channel, which tends to reduce the heat intensity on the anode surface. The melting of the cathode is, however, delayed because it absorbs slow moving ions. Moreover, the plasma radius at the cathode is smaller because it emits electrons. Hence the heating of the cathode is over a smaller area and thus more intense. This difference of spark behaviour at the cathode and the anode results in more material being removed from the cathode than from the anode and is the rationale for choosing the work piece as the cathode in coarse machining operation. Fig 1.3 (a) shows a die-sinking type EDM.

1.4.2 Wire-cut EDM:

It uses a continuously circulating metallic wire (typical diameter 0.1 mm, generally in steel, brass or copper), which cuts the work piece along a programmed path. Deionized water is used as dielectric, directly injected around the wire. The wire is capable of achieving very small cutting angles. The wire in wire-EDM applications acts almost like an electrical saw. The quality of the machining, i.e. precision and surface rugosity, is directly related to the discharge parameters (current, voltage, discharge duration, polarity), and also on the dielectric cleanliness. Sparks with strong current produce deep craters: a high removal rate is obtained but with a high surface rugosity. On the other hand, sparks with low current will produce small craters: the surface rugosity is low but the removal rate is also low. Fig.1.3 (b) shows a wire-cut EDM.

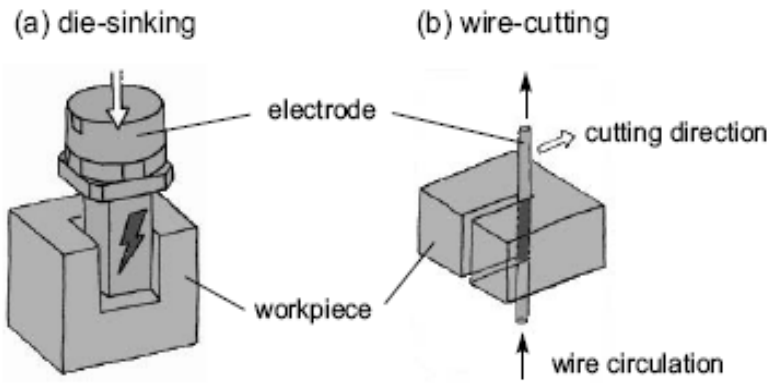

(a) Die-sinking EDM (b) Wire-cut EDM

Fig.1.3 Types of EDM

1.4.3 Equipments of EDM:-

Major subassemblies of the process are:-

(a) Power Supply: It transforms the alternating current from the main utility electrical supply to pulse DC required to produce spark discharges at the machining gap.

(b) Dielectric system: The dielectric system consists of dielectric fluid, delivery device, pumps, and filters.

(c) Electrode: It is the tool determining shape of the cavity generated. It depends upon material & design. Requirements for selection: should be readily available, easily machinable, exhibit low wear, electrically conductive & provide good surface finish.

(d) Servo System: It is Commanded from signals of gap voltage sensor system in power supply& controls the infeed of electrode or work piece to match material removal.

1.5 EDM PARAMETERS:

Parameters in EDM can be classified into three categories: control parameters, process result, and sensing parameters. The complete set of parameters is machine dependent. Different

EDM machines have different set of parameters due to the difference in their designs. A list of parameters usually found on most EDM machines is given in Table 1.1. Control parameters and process results are discussed below. Control parameters include those related to the work piece, tool electrode, generator, servo system, dielectric system, and the NC unit. Some of these parameters are fairly straight-forward and require no further explanation.

1.5.1 Generators

Generator or power supply provides electrical energy in the form of pulses to the working gap. Generators can be roughly classified into two categories: RC-relaxation generators and static pulse generators. RC-relaxation generators use charging circuitry to charge parallel capacitors to the gap. Discharges occur when the voltage across the gap reaches a certain level. The control parameters on generator are most important because they directly determine the power applied to the working gap.

a) Open-circuit Voltage: Open-circuit voltage specifies the voltage of applied pulses. It is not the voltage across the gap during electrical discharges. The latter is always about 15~25V.

b) Pulse Duration or Discharge Duration: These parameters determine the length of the applied voltage pulses. Pulse duration, which is a setting on iso-frequent generators, sets the length of applied voltage pulses. During pulse duration, the lengths of ignition delay and discharge duration depend on the gap state. The actual discharge duration is not controllable. In iso-energetic generators, discharge duration can be set directly. Together with peak discharge current, pulse duration sets the amount of energy generated during a single electrical discharge.

c) Peak Discharge Current: The setting of peak discharge current on static pulse generators generally determines the number of power units connected parallel to the gap rather than the exact current level. The larger peak discharge current means the higher power intensity during electrical discharge.

d) Pulse Interval, Duty Factor, or Pulse Frequency: Pulse interval, duty factor, or pulse frequency determines the separation of pulses. Duty factor is defined as the ratio of pulse duration over

pulse period. In machines with duty factor setting, pulse interval is set indirectly by setting pulse duration and duty factor. Pulse frequency is also used to set the pulse interval on some machines.

e) Polarity: It specifies the polarity of work piece and tool electrode. Depending on the application, the polarity can be either way.

1.5.2 Servo System

The servo system controls the tool motion relative to the work piece to follow the desired path. It also controls the gap width within such a range that the discharge process can continue. If tool electrode moves too fast and touches the work piece, short circuit occurs. Short circuit contributes little to material removal because the voltage drop between electrodes is small and the current is limited by the generator. If tool electrode moves too slowly, the gap becomes too wide and electrical discharge never occurs. Another function of servo system is to retract the tool electrode when deterioration of gap condition is detected. The width cannot be measured during machining; other measurable variables are required for servo control. The ignition delay affects the average gap voltage; both average ignition delay and average gap voltage are usually used as the indirect measurement of gap width. The servo reference voltage and reference average ignition delay set the reference values for servo control.

1.5.3 Dielectric System

The liquid dielectric plays a crucial role during the whole process:
(a) It cools down the electrodes.
(b) It guarantees a high plasma pressure and therefore a high removing force on the molten metal when the plasma collapses.
(c) It solidifies the molten metal into small spherical particles.
(d) It also flushes away these particles.

The most widely used types of dielectric liquid are mineral hydro-carbon oil for die-sinking EDM and deionized water for wire-cut EDM. The post-discharge is in fact a crucial stage, during which the electrode gap is cleaned of the removed particles for the next discharge.

If particles stay in the gap, the electrical conductivity of the dielectric liquid increases, leading to a bad control of the process and poor machining quality. To enhance the flushing of particles, the dielectric generally flows through the gap. In addition, the electrode movement can be pulsed, typically every second, performing a large retreat movement. This pulsing movement also enhances the cleaning, on a larger scale, by bringing "fresh" dielectric into the gap.

1.5.4 Material Removal

Material removal determines both machining rate and tool electrode wear. In die sinking EDM, the material removal rate is defined as removed volume per unit time and specifies material removal on work piece. The relative tool wear, defined as the volumetric ratio of material removal on tool electrode over that on work piece, measures the material removal on tool electrode. The ratios of material removal between electrodes depend on some of the control parameters. Current density has the greatest influence on power distribution, which determines the ratio of material removal between electrodes. The plasma channel expands during discharge duration; the pulse duration is the most important control parameter affecting the relative material removal rate between the electrodes. The anode has larger material removal with shorter pulse duration while the cathode has larger material removal with longer pulse duration. Besides pulse duration, parameters that cause decrease of current density can reduce the material removal of the anode, too [7].

Some of the most important parameters implicated in the EDM manufacturing process for Material Removal Rate (MRR) are the following ones:-

(a) On-time (pulse time or t_i): It is the duration of time for which the current is allowed to flow per cycle. Material removal is directly proportional to the amount of energy applied during this on-time. This energy is controlled by the peak current and the length of the on-time.

(b) Off-time (pause time or t_0): It is the duration of time between the sparks (T_{on}). This time allows the molten material to solidify and to be wash out of the arc gap. This parameter affects the speed and the stability of the cut. Thus, if the off-time is too short, it will cause unstable sparks.

(c) Arc gap (or gap): It is the distance between the electrode and the part during the process of EDM. It may be called as spark gap.

(d) Duty cycle: It is the percentage of on-time relative to the total cycle time. This parameter is calculated by dividing the on-time by the total cycle time [8].

1.5.5 Surface Integrity

The electrode surface machined by EDM can be characterized by geometrical shape of the surface, metallurgical and chemical characteristics, and mechanical properties of the superficial area. Surface roughness is reported to increase with discharge energy [9]. The thermal actions of the sparks produce a surface layer that consists of resolidified layer on the top of heat-affected-zone. Metallurgical, chemical, and mechanical changes exist in this surface layer. The machined surface is made up of three distinctive layers consisting of white layer/recast layer, heat affected zone (HAZ) and unaffected parent metal. The thickness of the recast layer formed on the work piece surface and the level of thermal damage suffered by the electrode can be determined by analyzing the growth of the plasma channel during sparking. Since the white layer is the topmost layer exposed to the environment, it exerts a great influence on the surface properties of the work piece. Lately, powders are suspended in the dielectric fluid to facilitate the ignition process by creating a higher discharge probability and lowering the breakdown strength of the insulating dielectric fluid. As a result, it increases the MRR, reduces the TWR and improves the sparking efficiency producing a strong corrosion resistant EDMed surface [10]. Moreover, the presence of powders in the dielectric fluid increases the micro-hardness and reduces the micro-cracks on the EDMed surface due to a reduction of losing alloying elements residing onto the work piece.

1.5.6 Geometrical Accuracy

There is a gap between the work piece and the tool electrode during the EDM process. This gap as well as the tool wear makes the resultant machined work piece shape different from the theoretical one. Such deviation needs to be compensated by undersize tool electrode and by setting the correct tool feed.

Table 1.1 List of parameters found on most EDM machines

Control Parameters	Process Parameters	Sensing Parameters
1. Work Piece - Material - Dimension - Geometrical Shape 2. Tool Electrode - Material - Tool Diameter 3. Generator - Open Circuit Voltage - Pulse Duration - Discharge Duration - Peak Discharge Current - Duty factor - Pulse Factor - Polarity 4. Servo System - Servo Reference Voltage - Reference Average Ignition Delay - Gain - Pulsation of Tool Electrode 5. Dielectric system - Dielectric type - Conductivity - Flushing Method - Flushing Rate	1. Material Removal - Work Piece MRR - Cutting Speed - Tool Electrode MRR - Wear 2. Geometrical Accuracy - Geometrical Shape of Work Piece - Aspect Ratio - 2D - 3D 3. Surface Integrity - Geometrical Shape of the Surface - Surface Roughness - Crater Shape 4. Metallurgical and Chemical Characteristics - Surface Layer - Material Transfer -Metallurgical Transformation - Chemical Diffusion 5. Mechanical Properties - Residual Stress - Micro Hardness - Micro Cracks	1. Electrical Parameters - Pulse Type - Ignition Delay - Average Gap Voltage -Average Discharge Voltage -Average Discharge Current - Voltage Fall time - Power Dissipation - Sparking Frequency -Sum of Effective Discharge Duration Per Unit Time - Pulse Efficiency Index

1.6 CHARACTERISTICS OF EDM

1.6.1 Advantages of EDM

One of the main advantages of EDM is a consequence of the thermal process. It is based on: removing material by melting and evaporation, so the hardness of the work piece is no limitation for machining. Even the hardest steel grades can be machined with almost same machining speed as for softer steels.

a) Machining hard materials

The capability of machining hard materials is a major benefit as most tools and moulds are made of hard materials to increase their lifetime. The recent developments in cutting tools for turning and milling and the processes of high speed machining allow to machine harder materials than before, but EDM still remains the only available process for machining many hard materials (e.g. carbides).

b) Absence of forces

As the EDM-process is based on a thermal principle, almost no mechanical forces are applied to the work piece. This allows to machine very thin and fragile structures. It should be noticed that some small mechanical, electrical and magnetic forces are produced by the EDM-process and that, as already mentioned, flushing and hydraulic forces may become large for some work piece geometry. The large cutting forces of the mechanical materials removal processes, however, remain absent.

c) Machining of complex shapes

Complex cavities can often be machined without difficulties by die-sinking EDM, provided an electrode is available, having the opposite shape of the cavity. In most cases, the soft electrode (Cu, graphite or W-Cu) can be machined rather easily by conventional processes as milling and turning or by wire-cutting EDM. In this way, complex cavities can be eroded, even on simple die-sinking machines which can only erode in the downward direction. Due to the modern NC control systems on die sinking machines, even more complicated work pieces can be machined. Modern, multi-axis NC controlled wire-cutting machines (where e.g. the wire inclination can be

constantly) also allow to achieve very intricate work pieces. Besides complex shapes, conventional processes, can easily be machined by EDM. EDM is also one of the only processes capable of machining three dimensional micro work pieces. A large growth of applications for so called micro electro mechanical systems (MEMS) is predicted for the near future.

d) High degree of automation

The high degree of automation and the use of tool and work piece changers allow the machines to work unattended for overnight or during the weekends.

e) Accuracy of the process

EDM is a process where very accurate structures can be machined (typically 1 to 5μm). In the case of work pieces with a higher thickness, the accuracy and the fine surface quality remains the same over the whole thickness of the work piece, due to the fact that EDM is machining with the same process conditions over the total work piece height. Process like laser beam or water jet machining can also achieve a high surface finish, but they can be used only for work pieces with a limited thickness. When the thickness increases, focusing problems induce a loss of quality. One of the main application fields of EDM is the mould and dies making industry. To achieve a high lifetime of the work piece, very hard materials should be used. The high hardness is often obtained by a thermal treatment. After the treatment however, most work pieces can no longer be machined by conventional processes, so EDM is the appropriate way to manufacture these work pieces.

1.6.2 Disadvantages of EDM

a) The need for electrical conductivity

To be able to create discharges, the work piece has to be electrically conductive. Isolators, like plastics, glass and most ceramics, can not be machined by EDM, although some exception like for example diamond is known. Machining of partial conductors like Si semi-conductors, partially conductive ceramics and even glass is also possible.

b) Predictability of the gap

The dimensions of the gap are not always easily predictable, especially with intricate work piece geometry. In these cases, the flushing conditions and the contamination state of differ from the specified one. In the case of die-sinking EDM, the tool wear also contributes to a deviation of the desired work piece geometry and it could reduce the achievable accuracy. Intermediate measuring of the work piece or some preliminary tests can often solve the problems.

c) Optimization of the electrical parameters

The choice of the electrical parameters of the EDM-process depends largely on the material combination of electrode and work piece and EDM manufactures only supply these parameters for a limited amount of material combinations. When machining special alloys, the user has to develop his own technology.

d) Low material removal rate

The material removal of the EDM-process is rather low, especially in the case of die-sinking EDM where the total volume of a cavity has to be removed by melting and evaporating the metal. With wire-EDM only the outline of the desired work piece shape has to be machined.

Due to the low material removal rate, EDM is principally limited to the production of small series although some specific mass production applications are known.

1.6.3 Applications of EDM:

(a) In the machining of very hard metals and alloys used in aerospace, automotive and nuclear industries.

(b) It is a promising technique to meet increasing demands for smaller components usually highly complicated, multi-functional parts used in the field of micro-electronics.

(c) Application potential of EDM can be further enhanced if its machining rates can be increased and resulting surface damage to the work piece is accurately estimated and reduced.

1.7 OBJECTIVE OF THE PRESENT WORK:

The objective of the present work is an attempt to determine the temperature distribution of tool and work piece by developing a thermal-electrical model for sparks generated by electrical discharge in a liquid media. The discharge channel being an electrical conductor will dissipate heat, which can be explained by the Joule Heating Effect. The amount of heat dissipated varies with the thermal-physical properties of the conductor. The model is to be developed by using ANSYS software. ANSYS uses the finite-element method to solve the underlying governing equations and the associated problem-specific boundary conditions. Material Removal Rate, Surface Roughness and the maximum temperature reached in the discharge channel is to be determined.

CHAPTER – 2

The earlier work related to the present research area by other researchers have been explored and the progressive account of the work has been enumerated in this chapter.

Drayl D.Bitonto et al. (1989) [11] presented a simple cathode erosion model for EDM process. This point heat-source model accepts power rather than temperature as the boundary condition at the plasma/cathode interface. A constant fraction of the total power supplied to the gap is transferred to the cathode over a wide range of currents. The model identifies the key parameters of optimum pulse time factor (g) and erodibility (j) in terms of thermo-physical properties of cathode material. The differences of macroscopic dielectric properties affect6 the microscopic mechanisms for energy transfer at cathode. The constancy of the fraction of power supplied to the cathode is assumed and obtained from a single current measurement.

Mukund R.Patel et al. (1989) [12] presented an erosion model for anode material. The model accepts power rather than temperature as boundary condition at plasma/anode interface. A constant fraction of the total power supplied to the gap is transferred to the anode. The power supplied is assumed to produce a Gaussian-distributed heat flux on the area of anode which grows with time. Rapid melting of anodic material and subsequent resolidification of the material for longer durations of time is presented.

P. Madhu et al. (1991) [13] proposed a model for predicting the material removal rate and depth of damaged layer during EDM. The transient heat conduction equation for the work piece which accounts for the heat absorption due to melting has been solved by Finite Element Method. Simulations have been performed for a single spark in the form of pulses. The width of crater and the depth of penetration depend on spark-radius and the power intensity. It was found that MRR increases with power per spark and decreases with an increase in computational machining cycle time. It increases immediately after machining starts but soon reaches a steady state value.

Philip T. Eubank et al. (1993) [14] developed a variable mass, cylindrical plasma model for sparks created by electric discharge in a liquid media. A thermo-physical property subroutine

allows realistic estimation of plasma enthalpy, mass-density and particle fractions by inclusion of the heats of dissociation and ionization for plasma created from deionized. Numerical solution of the model provides plasma radius, temperature, pressure and mass as a function of pulse time for fixed current, electrode gap and power fraction remaining in the plasma. High plasma temperatures and pressures persist in the plasma even after long pulse times. Uniquely high pressures found show that superheating is the dominant mechanism for EDM spark erosion.

Indrajit Basak et al. (1997) et al. [15] developed a simplified model to predict the characteristics of the material removal rate for varying input parameters with the objective of finding the possibility of enhancing the capability of the Electrochemical discharge machining process and it has been found that an extra control parameter can be obtained by introducing an additional inductance in the circuit. The theoretical and experimental results indicate that a substantial increase in the material removal rate can be achieved due to the additional inductance introduced.

J.C. Rebelo et al. (1999) [16] presented an experimental study on the effect of EDM parameters on material removal rate (MRR) and surface quality, when machining high strength copper-beryllium alloys. Processing parameters for rough, finishing and micro-finishing or polishing regimes were analysed. The surface integrity of electro-discharge machined is quantified by measuring the roughness values, crater diameter and white layer thickness. ``Thermal erosion models", as justification for the optimal setting of different EDM parameters and achievement of distinct surface integrity using materials with different thermal properties, are discussed. For positive polarity the EDMed samples presents a ``normal" behaviour with increasing MRR when machining energy is increased. However, for negative polarity, carbon is attracted by the work piece surface causing a deleterious effect on surface quality and MRR. The surface roughness for rough and finishing regimes increases with both discharge current and on-time.

C.H. Che Haron et al. (2001) [17] determined the possible correlation between the EDM parameter (current) and the machinability factors (material removal rate and electrode wear rate). The material removal rate of the work piece material and the wear rate of electrode material were obtained based on the calculation of the percentage of mass loss per machining time. It was

found that the material removal rate and electrode wear rate were dependent on the diameter of the electrode and had a close relation with the supply of current. Low current was found suitable for small diameter electrode while high current for large diameter of electrode.

A. Kulkarni et al. (2002) [18] attempted to identify the underlying mechanism of the electrochemical discharge machining process through experimental observations of time-varying current in the circuit. Based on these observations the basic mechanism of temperature rise and material removal is proposed. They found the discharge is a discrete phenomenon. The breakdown is similar to the one that occurs in a gas due to a large electric field of the order of 10^7 V/m which gets generated locally.

Vinod Yadav et al. (2002) [19] proposed that the high temperature gradients generated at the gap during EDM result in large localized thermal stresses in a small heat-affected zone leading to micro-cracks, decrease in strength and fatigue life and possibly catastrophic failure. A finite element model has been developed to estimate the temperature field and thermal stresses. The effects of various process variables (current and duty cycle) on temperature distribution and thermal stress distribution have been reported. After one spark, substantial compressive and tensile stresses develop in a thin layer around the spark location and the thermal stresses exceed the yield strength of the work piece mostly in an extremely thin zone near the spark.

Kesheng Wang et al. (2003) [20] discussed the development and application of a hybrid artificial neural network and genetic algorism methodology to modelling and optimisation of EDM. The hybridisation approach aims at exploiting the strong capabilities of the two tools and at solving manufacturing problems that are not amenable for modelling using traditional methods. The developed methodology with the model is highly beneficial to manufacturing industries, such as aerospace, automobile and tool making industries. The solutions achieved establish better knowledge about the interaction between the tool and the work piece.

H.T. Lee et al. (2003) [21] presented a study of the relationship between EDM parameters and surface cracks by using a full factorial design, based upon discharge current and pulse-on time parameters on D2 and H13 tool steels as materials. The formation of surface cracks is explored by considering surface roughness, white layer thickness, and the stress

induced by the EDM process. Its use will provide a valuable aid in improving the quality of the EDM process. Increased pulse-on duration will increase both the average white layer thickness and the induced stress. These two conditions tend to promote crack formation. When the pulse current is increased, the increase in material removal rate causes a high deviation of thickness of the white layer. Compared to a thin white layer, a thick white layer has a tendency to crack more readily.

Josko Valentincic et al. (2004) [22] proposed that rough machining parameters have to be selected according to the size of the eroding surface to achieve a high removal rate and low electrode wear. The size of the eroding surface varies according to the depth of machining and it has to be determined online. The work presented shows that the electric current signal depends on the size of the eroding surface. To detect the size of the eroding surface based on the electric current signal in the gap, it is necessary to build a different model for each machining regime. For constant machining parameters and varying size of the eroding surface , the attributes of the electric current signal were acquired and used as inputs to the modeller; a conditional average estimator (CAE) was used as a non parametric regression modeller.

B. Lauwers et al. (2004) [23] presents a detailed investigation of the material removal mechanisms of some commercially available electrical conductive ceramic materials through analysis of the debris and the surface/sub-surface quality. ZrO_2-based, Si_3N_4-based and Al_2O_3-based ceramic materials, with additions of electrical conductive phases like TiN and TiCN, have been studied. They pointed out that besides the typical EDM material removal mechanisms, such as melting/evaporation and spalling, other mechanisms can occur such as oxidation and dissolution of the base material. The formation of cracks depends among factors like thermal conductivity of the material, melting point and strength, on the fracture toughness of the material.

Shankar Singh et al. (2004) [24] reported the results of an experimental investigation carried out to study the effects of machining parameters such as pulsed current on material removal rate, diameteral over cut, electrode wear, and surface roughness in electric discharge machining of En-31 tool steel (IS designation: T105 Cr 1 Mn 60) hardened and tempered to 55 HRc. The work material was ED machined with copper, copper tungsten, brass and aluminium

electrodes by varying the pulsed current at reverse polarity. Investigations indicate that the output parameters of EDM increase with the increase in pulsed current and the best machining rates are achieved with copper and aluminium electrodes. Copper is comparatively a better electrode material as it gives better surface finish, low diameteral over cut, high MRR and less electrode wear for En-31 work material, and aluminium is next to copper in performance, and may be preferred where surface finish is not the requirement.

Leonid I. Sharakhovsky et al. (2006) [25] modified the step-wise model (SWM) of cold electrodes erosion of electric arc heaters for the calculation of work piece removal rate in EDM process. Modified model applies both relations the step-wise erosion model and the point heat source erosion model and takes into account the discharge current, the discharge pulse/pause time and thermo physical properties of machined material. The great advantage of the model is that by using the results of single experiment and obtaining the effective enthalpy it is possible to calculate WRR for given work piece material and dielectric at arbitrary working regimes.

Nizar Ben Salah et al. (2006) [26] presented numerical results concerning the temperature distribution due to electric discharge machining process. From these thermal results, the material removal rate and the total roughness were deduced and compared with experimental observations. The temperature variation of conductivity was taken into account and shown that it is of crucial importance and gives the better correlations with experimental data.

K.L. Bhondwe et al. (2006) [27] proposed a thermal model for the calculation of material removal rate during ECSM. The temperature distribution within zone of influence of single spark is first obtained with the application of finite element method .The nodal temperatures are further post processed for estimating MRR. Further the parametric studies are carried out for different parameters like electrolyte concentration, duty factor and energy partition. The increase in MRR is found to increase with increase in electrolyte concentration due to ECSM of soda lime glass work piece material. The change in the value of MRR for soda lime glass with concentration is found to be more than that of alumina. MRR is found to increase with increase in duty factor and energy partition for both soda lime glass and alumina work piece.

J. Marafona et al. (2006) [28] developed a thermal-electrical model for sparks generated by electrical discharge in a liquid media. The radii value of the conductor is a function of the current intensity and pulse duration. The thermal–physical values used in the model are the average of both the ambient and melting value. Copper and iron are the materials used for anode and cathode, respectively. The Finite Element Analysis (FEA) results were compared with the experimental values of the table of AGIE SIT used by other researchers. The Joule heating effect is considered not only in the EDM electrodes but also in the discharge channel, which is considered by the authors as the driving phenomenon of the EDM process.

Philip Allen et al. (2007) [29] presented the process simulation and residual stress analysis for the micro-EDM machining on molybdenum. Material removal is analyzed using a thermo-numerical model, which simulates a single spark discharge process. Using the numerical model, the effects of important EDM parameters such as the pulse duration on the crater dimension and the tool wear percentage are studied. The model estimates that the percentages of tool wear decreases with an increase in the pulse duration. The FEM study indicates that tensile residual stresses build up near the crater boundary in all directions during the micro-EDM process leading to micro-cracks.

Against this background, present research work has been undertaken to develop a thermal-electrical model for sparks generated by electrical discharge in a liquid media. Attempts have been made in this work to determine the temperature distribution of tool, work piece and the discharge channel using Finite element Method. It will continue to be an important area of concern in coming years. The present investigation is a step in this direction.

CHAPTER – 3

The governing equations for the finite element method used in the model analysis have been depicted in this chapter. The element selection, assumptions made and simulation procedure has also been presented.

The thermal erosion theory is the most accepted mathematical model for evaluating material removal from electrodes during EDM process. It postulates that the process involves melted electrode and its evaporation by the discharge energy dissipated on electrode surface. Part of the melted and evaporated material is then ejected from electrode by force of different natures. Many researchers analyzed the material removal by heat conduction models with a heat source acting on the surface of electrode during a single electrical discharge [7]. The phenomena analyzed include power distribution during electrical discharge, the melting and boiling isothermals on the electrode, and material ejection from the electrode. The energy generated by electrical discharge is allocated at the anode, the cathode, and the plasma column. The knowledge about this power distribution is required for the application of heat conduction model. The temperature rise of electrodes due to dissipated discharge energy is calculated to determine the melting and boiling isothermals at the electrodes.

3.1 FEA FORMULATION:

Joule heating arises when the energy dissipated by an electrical current flowing through a conductor is converted into thermal energy. Coupling arises from two sources: the conductivity in the electrical problem is temperature dependent, and the internal heat generated in the thermal problem is a function of electrical current [28]. The thermal part of the problem includes all the heat conduction and heat storage (specific and latent heat); forced heat convection caused by fluid flowing through the mesh is not considered. The thermal–electrical elements have both temperature and electrical potential as nodal variables.

3.1.1 Governing Equation

The electric field in a conducting material is governed by Maxwell's equation of conservation of charge.It states that the divergence of the current density is equal to the negative rate of change of the charge density.

$\nabla .J = -\delta\rho / \delta t$

Assuming steady-state direct current,

$I = dQ / d t$

$r_c = dQ / dVdt$

$$\int_v r_c \, dV = \int dI = \int_s \mathbf{J.n} \, ds \qquad (1)$$

So, the equation reduces to:

$$\int_s \mathbf{J.n} \, ds = \int_v r_c \, dV \qquad (2)$$

where V is any control volume whose surface is S, **n** is the outward normal to S, **J** is the electrical current density (current per unit area), and r_c is the internal volumetric current source per unit volume [19].

The divergence theorem can be used to convert the surface integral into volume integral:

$$\int_v \nabla .J \, dV = \int_s \mathbf{J.n} \, ds \qquad (3)$$

Using equation (1), equation (3) becomes:

$$\int_v \nabla .\mathbf{J} \, dV = \int_v r_c \, dV \qquad (4)$$

Since $\nabla = \hat{i} \frac{\partial}{\partial x} + \hat{j} \frac{\partial}{\partial y} + \hat{k} \frac{\partial}{\partial z}$

Here the component of current along $\hat{i}$ direction

$$\int_v (\hat{i} \frac{\partial}{\partial x} + \hat{j} \frac{\partial}{\partial y} + \hat{k} \frac{\partial}{\partial z}).i \, \mathbf{J} \, dV = \int r_c \, dV$$

$$\int_v \frac{\partial}{\partial x} \mathbf{J} \, dV = \int_v r_c \, dV$$

$$[\frac{\partial}{\partial x}\mathbf{J}- r_c\ ]\ dV = 0 \qquad (5)$$

since the volume is arbitrary, this provides the point wise differential equation:

$$\frac{\partial}{\partial x}\mathbf{J}- r_c = 0 \qquad (6)$$

The equivalent weak form is obtained by introducing an arbitrary variational, the electrical potential field, δφ, and integrating over the volume:

$$\int_v d\varphi\ [\frac{\partial}{\partial x}\text{-}\mathbf{J}- r_c\ ]\ dV = 0 \qquad (7)$$

$$\int_v - (\frac{\partial}{\partial x}\mathbf{J}\ \delta\varphi\ dV - r_c\ \ \delta\varphi\ dV) = 0 \qquad (8)$$

$$\int_v - (\frac{\partial \delta\varphi}{\partial x}\mathbf{J}\ dV + \delta\delta\varphi\frac{\partial}{\partial x}\mathbf{J}\ dV - r_c\delta\ \varphi\ dV) = 0 \qquad (9)$$

Since **J** defined as **–J.n** is the current density entering the control volume across S.

$$-\int_v \frac{\partial \delta\varphi}{\partial x}\mathbf{J}\ dV- \delta\varphi\int_v \nabla .\mathbf{J}\ dV - \int_v r_c\,\delta\varphi\ dV \qquad (10)$$

$$-\int_v \frac{\partial \delta\varphi}{\partial x}\mathbf{J}\ dV- \delta\varphi\int_s \mathbf{J}\ ds -\int_v r_c\,\delta\varphi\ dV = 0 \qquad (11)$$

$$-\int_v \frac{\partial \delta\varphi}{\partial x}\mathbf{J}\ dV =\int_s \delta\varphi\ \mathbf{J}\ ds + \int_v \delta\varphi\ r_c\ dV \qquad (12)$$

3.1.2 Constitutive Behaviour

The flow of electrical current is described by Ohm's law

$$J = \boldsymbol{\sigma}^{E}.E \qquad (13)$$

Where $\boldsymbol{\sigma}^{E}$ (θ,f^{α}) is the electrical conductivity matrix; q is the temperature; and f^{α} , α=1, 2,…., are any predefined field variables.

The conductivity can be isotropic, orthotropic, or fully anisotropic.

E(x) is the electrical field intensity defined as:

$$E= - \frac{\partial \varphi}{\partial x} \qquad (14)$$

Since a potential rise occurs when a charged particle moves against the electrical field, the direction of the gradient is opposite to that of the electrical field.

Using this definition of the electrical field, Ohm's law is rewritten as:

$$J = - \boldsymbol{\sigma}^{E} . \frac{\partial \varphi}{\partial x} \qquad (15)$$

The constitutive relation is linear; that is, it assumes that the electrical conductivity is independent of the electrical field.

Introducing Ohm's law, the governing conservation of charge equation (12) becomes:

$$\int_{v} \frac{\partial \delta\varphi}{\partial x} . \boldsymbol{\sigma}^{E} . \frac{\partial \varphi}{\partial x} \, dV = \int_{v} r_c \, \delta\varphi \, dV + \int_{s} \delta\varphi \, \mathbf{J} \, ds \qquad (16)$$

3.1.3 Thermal Energy Balance

The heat conduction behaviour is described by the basic energy balance relation

$$\int_{v} \rho \dot{U} \, \delta\theta dV + \int_{v} \frac{\partial \delta\theta}{\partial x} .k \frac{\partial \theta}{\partial x} .dV = \int_{v} \delta\theta r \, dV + \int_{s} \delta\theta q \, dS \qquad (17)$$

where V is a volume of solid material, with surface area S; r is the density of the material; U is the internal energy; k is the thermal conductivity matrix; q is the heat flux per unit area of the body, flowing into the body; and r is the heat generated within the body.

Equations (16) and (17) describe the electrical and thermal problems, respectively.

Coupling arises from two sources:

The conductivity in the electrical problem is temperature dependent, $\boldsymbol{\sigma}^{E} = \boldsymbol{\sigma}^{E}(\theta)$, and the internal heat generation in the thermal problem is a function of electrical current, $r = r_{ec}$ (J), as described in equation (18).

3.1.4. Thermal energy due to electrical current

Joule's law describes the rate of electrical energy, Pec, dissipated by current flowing through a conductor as

$$P_{ec} = \mathbf{E.J} \qquad (18)$$

Using Equations ( ) and ( ), Joule's law is rewritten as:

$$P_{ec} = \mathbf{E}.\ \boldsymbol{\sigma}^{E}.\mathbf{E} \qquad (19)$$

In a steady-state analysis Pec is evaluated at time t+Δt. In a transient analysis an averaged value of Pec is obtained over the increment.

3.1.5. Surface conditions

The surface S of the body consists of parts on which boundary conditions can be prescribed, S_p, and parts that can interact with nearby surfaces of other bodies, S_i. Prescribed boundary conditions include the electrical potential, φ= φ(x,t); temperature, θ= θ(x,t); electrical current density, J=J(x,t); heat flux, q=q(x,t); and surface convection and radiation conditions. The surface interaction model includes heat conduction and radiation effects between the interface surfaces and electrical current flowing across the interface.

Heat conduction and radiation are modeled by:

$$q_c = k_g\ (\theta_B - \theta) \qquad (20)$$

and

$$q_r = F_B\ (\theta_B - \theta^z)^4 - F\ (\theta_B - \theta^z)^4 \qquad (21)$$

respectively, where θ is the temperature on the surface of the body under consideration,

θ_B is the temperature on the surface of the other body, θ^z is the value of absolute zero temperature on the temperature scale being used; kg $(\bar{\theta}, \bar{f}^{\alpha})$ is the gap thermal conductivity,

$\bar{\theta}$ = (1/2) (θ+ θ_B) is the average interface temperature, $\bar{f}^{\alpha} = (1/2)(f_A^{\alpha} + f_B^{\alpha})$ is the average of any predefined field variables at A and B, and F and F_B are constants.

The electrical current flowing between the interface surfaces is modeled as:

$$J = \sigma_g\ (\varphi_B - \varphi) \qquad (22)$$

where φ is the electrical potential on the surface of the body under consideration, φB is the electrical potential on the surface of the other body, and σ_g $(\bar{\theta}, \bar{f}^{\alpha})$ is the gap electrical conductivity. The electrical energy dissipated by the current flowing across the interface,

$$P_{ec} = J\,(\varphi_B - \varphi) = \sigma_g\,(\varphi_B - \varphi)^2 \qquad (23)$$

is released as heat on surfaces of bodies.

$$q_{ec} = f\,\eta_g\,P_{ec} \qquad (24)$$

and

$$q^{B}_{ec} = (1\text{-}f)\,\eta_g\,P_{ec} \qquad (25)$$

where η_g is an energy conversion factor and f specifies how the total heat is distributed between the interface surfaces. P_{ec} is evaluated at the end of the time increment in a steady state analysis, and an averaged value over the time increment is used in a transient analysis.

Introducing the surface interaction effects and electrical energy released as thermal energy, the governing electric and thermal equations become:

$$\int_v \frac{\partial\delta\varphi}{\partial x}\,.\,\boldsymbol{\sigma}^{E}\,.\,\frac{\partial\varphi}{\partial x}\,dV = \int_v r_c\,\delta\varphi\,dV + \int_{Sp} \delta\varphi\,\mathbf{J}\,ds + \int_{Si} \delta\varphi\,\sigma_g\,(\varphi_B - \varphi)\,dS \qquad (26)$$

and

$$\int_v \rho\dot{U}\,\delta\theta dV + \int_v \frac{\partial\delta\theta}{\partial x}.k\frac{\partial\theta}{\partial x}.dV = \int_v \delta\theta r\,dV + \int_v \delta\theta\,\eta_g\,P_{ec}\,dV + \int_{Sp} \delta\theta q\,dS + \int_{Si} \delta\theta\,(q_c + q_r + q_{ec})\,dS \qquad (27)$$

3.1.6. Spatial Discretization

In a finite element model equilibrium is approximated as a finite set of equations by introducing interpolation functions. Discretized quantities are indicated by uppercase superscripts (for example, φ^N). The discretized quantities represent nodal variables, with nodes shared between adjacent elements and appropriate interpolation chosen to provide adequate continuity of the assumed variation. The virtual electrical potential field is interpolated by:

$$\delta\varphi = N^N\,\delta\varphi^N \qquad (28)$$

where N^N are the interpolation functions. Substituting Equation (28) in Equation (26) we obtain a discretized electrical equation.

The temperature field in the thermal problem is approximated by the same set of interpolation functions:

$$\delta\theta = N^P \, \delta\varphi^p \qquad (29)$$

Using these interpolation functions and a backward difference operator to integrate the internal energy rate, $\dot{U}$, the thermal energy balance relation is obtained, transforming the energy balance Equation (27) in a discretized one.

3.2 DISCHARGE CHANNEL RADIUS:

According to Erden [30] the discharge channel is influenced by the dielectric and electrode materials. This is extremely difficult to prove due to very short pulse duration. The Equation (30), obtained by Erden, can be used to calculate the radius in EDM process, and is discharge power and time dependent.

$$R(t) = K \, Q^m \, t^n \qquad (30)$$

where Q is discharge power and m, n and K are empirical constants.
However, some authors [12, 19] used Equation (31) to calculate the plasma radius which is only time-dependent. The empirical constants n and K are equal to 0.75 and 0.788, respectively.

$$R(t) = K \, t^n \qquad (31)$$

Equation (32) is given by Pandey and Jilani [31] to calculate the discharge radius in the EDM process.

$$Tb = (E_0 R / K\pi^{0.5}) \tan^{-1} [4\alpha t / R^2]^{0.5} \qquad (32)$$

where Tb is the boiling temperature, E_0 is the energy density and α is the thermal diffusivity. Van Dijck [28] has studied the variation of the removed material from the electrodes using different values of the discharge channel radius. As was shown, there are a large number of different equations used to calculate the discharge radius in the EDM process although these have restricted application.

Ikai and Hashiguchi [32] showed that the discharge radius is related to the current intensity and pulse duration as in Erden's Equation [30]. Marafona et.al [28] chose the discharge radius based on the work of Ikai and Hashiguchi among all the possibilities shown. This is called the equivalent heat input radius [R], which substitutes the radius changing of the heat supply. The equivalent heat input radius, which is dependent of the current intensity (I) and pulse duration (t), is thereby:

$$[R] = 2.04 \times 10^{-3} I^{0.43} t^{0.44} \quad (33)$$

This is a virtual radius that is used as the equivalent heat input radius. The importance of this assumption to the present research is to get a 'static' thermal–electrical model where a constant radius is used, different for each input current intensity case.

In the present work, an assumption has been made that the radius of the electrode is 20 times larger than the discharge channel radius.

Based on these equations, the present work was carried out. In order to model single shot discharge, a thermal –electric analysis was performed.

3.3 ASSUMPTIONS:

In previous study [13] was mentioned that EDM is physically similar to many gas discharges in which a constant current is passed through the plasma. The electrical discharge in the EDM process is of high complexity and uncertainty nature; so in order to simplify the mathematical model were done the following assumptions:

(1) The domain is considered as axisymmetric.
(2) In the present work the electrode radius is considered about 20 times larger than the discharge channel radius and the outer cylinder is adiabatic.
(3) The discharge channel is a uniform cylindrical shape.
(4) The EDM discharge is made in a vaporized medium in which a constant current passes through it.
(5) There is a partial conversion of the electrical in thermal energy-Joule heating-in the discharge channel.
(6) The work piece and tool are homogeneous and isotropic.

(7) The material properties of the electrodes and dielectric are temperature-independent.

(8) Averaged values of its thermal physic properties are used.

(9) The heat transferred to the electrodes occurs by conduction.

(10) In the discharge channel, there is no variation in the electrical potential in the radial direction.

(11) The analysis is done for a single discharge.

3.4 SIMULATION CONDITION AND PROCEDURE

For a single discharge test, copper and En-19 was used as specimens. The copper is used widely with the electrode material. The single discharge analysis procedure employs the commercial finite element code ANSYS Multiphysics to determine both temperature distribution and deformation of molten material by plasma pressure. ANSYS is a generally used finite element code to solve engineering problem [33]. The thermal analysis was performed when the electrical discharge machining conditions and the material properties were given. The heat flux intensity varied with discharge gap current trace and the diameter of plasma. During the discharge on-time, the melting region and the evaporating region were found. The material was assumed that certain part whose temperature goes over the evaporating point would be removed. The molten material consequently would be protruded up to crater edge. Figure 3.1 shows the plasma channel developed during on-time.

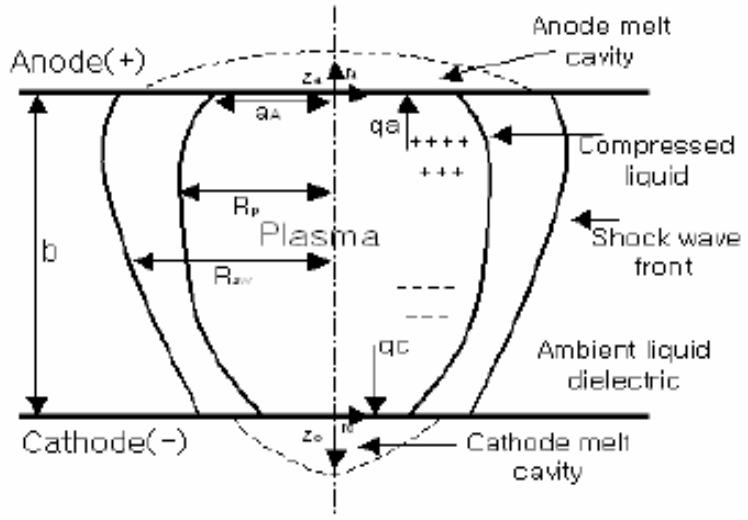

Fig. 3.1 Plasma channel developed during on-time

3.4.1 Element type for the analysis procedure:

Table 3.1 shows the element types considered for the model analysis [33].

Table 3.1 Element types used for the generation of model

Analysis	Element Type
Thermal-electric Coupling	2-D, Plane -67
Thermal-electric Coupling	2-D, Plane -67
Thermal-electric Coupling	2-D, Plane-67

3.4.2 Material Properties and applied Boundary conditions:

Material properties for the tool, work piece and discharge channel was set as input values.The boundary conditions were given as nodal variables. Based on the governing equations, the loading conditions applied were temperature and voltage which varied between nodes. Considering these properties the simulation was carried out for a single discharge. Actual EDM cycle consists of OFF Time and On Time. In this model, the process is assumed to be having a continuous sparking for a long period of computational machining cycle time (i.e. zero off time).

Table3.2 shows the material properties set for copper, En-19 and the EDM oil used as the dielectric fluid during the theoretical analysis.

Table 3.2 Material Properties for FEA

Material Property	Copper (cathode)	EDM Oil (dielectric)	En-19 (anode)
Density (g/mm^3)	8920×10^{-6}	5.7×10^{-8}	7700×10^{-6}
Conductivity (W/mmK)	400×10^{-3}	0.06	222×10^{-12}
Resistivity (Ω-mm)	1.7×10^{-11}	1	22.2×10^{-11}
Specific heat (J/gK)	385×10^{-3}	15	473×10^{-3}

The model was developed by selecting the element types and then assigning the attributes to the elements. Meshing was done and elements were created as shown in Fig.3.2. The figure also shows the loads applied and the boundary conditions given for the model generation. The model is considered to be symmetric about Z-axis.

Thermal Boundary Condition:

The temperature in the upper surface of the tool and lower surface of the work piece is 50˚C. The other surfaces in the boundary are condistered to be adiabatic.

Electrical Boundary Condition:

The voltage applied to the upper boundary of tool is 25V and that of the lower boundary of the work piece is 0V.

Then the solution was carried out and the temperature profile reached in the electrodes and discharge channel was obtained. The maximum surface roughness (R_{max}) values were also calculated.

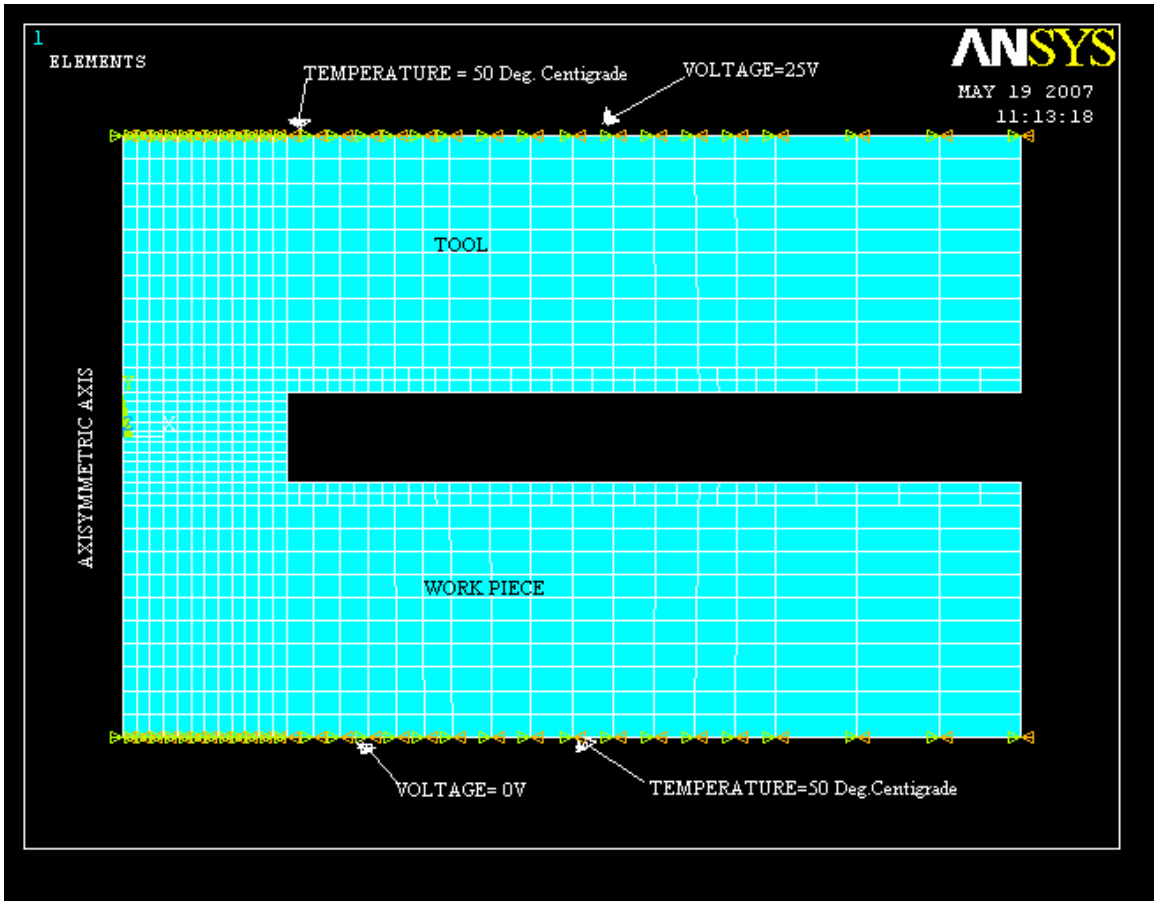

Fig.3.2 Elements after meshing and application of loads

CHAPTER – 4

This chapter deals with the experimental details and procedure followed for the machining and estimation of material removal rate.

The Electric Discharge Machine, model ELECTRONICA- ELECTRAPULS PS 50ZNC (die-sinking type) with servo-head (constant gap) and positive polarity for electrode was used to conduct the experiments. Commercial grade EDM oil (specific gravity= 0.763, freezing point= 94˚C) was used as dielectric fluid. Experiments were conducted with positive polarity of electrode. The pulsed discharge current was applied in various steps in positive mode. Fig.4.1 shows the EDM machine used for the experiment.

The electrode made up of copper was machined in cylindrical shape on a lathe machine and brazed with mild steel. Diameter of the electrode was 30mm and thickness 40mm. The work piece material is En-19 with diameter 50mm and thickness 10 mm. All surfaces were ground finished. The initial weight of the work piece material was measured. Fig.4.2 shows the electrode and work piece material during the machining operation.

The chemical composition of the work material is given in Table 4.1 [34].

Table 4.1 Chemical composition of En-19

Elements	Composition (wt. %)
C	0.35 – 0.45
Si	0.10 – 0.35
Mn	0.50 – 0.80
P max	0.050
S max	0.050
Cr	0.90 – 1.50
Mo	0.20 – 0.40

Fig. 4.1 EDM machine used for the experiment

Fig. 4.2 Electrode and work piece material used in the experiment

AISI-SAE (US Designations for steels) has given the classification to En-19 as 4140 Cr-Mo steel [35]. The older British specifications for steels have the letter En followed by a number where the last two digits stand for the carbon content. This series of Cr-Mo steels contain about 1% Cr with (0.15-0.25%) Mo. It enjoys great popularity because it is relatively cheap and possesses deep-hardening characteristics, ductility and weldability. Chromium is strong carbide forming element and its addition to steel increases its wear resistance and hardenability [36]. The beneficial effects arising from the presence of Cr in steels are enhanced by addition of molybdenum. The major applications of En-19 are:

(a) They are extensively used for pressure vessels, aircraft structural parts, automobile axles, steering knuckles and arms. They are also used for parts of heavier section.
(b) They are used for manufacture of springs, engine bolts, studs, axles, dies, rolls, tools, plates etc.
(c) These are suitable for the manufacture of ball bearings and crushing machinery.
(d) They are also employed in the making of cutlery steel and surgeon's blade.

Disadvantages:

(a) These steels show embrittlement (inter granular fracture) when tempered in the range of 500-575˚C because the transition temperature is raised.
(b) They also show surface markings.

Electric Discharge Machining is a process of repetitive sparking cycles. The figures representing the sparking cycles are shown in Fig4.3 and 4.4.

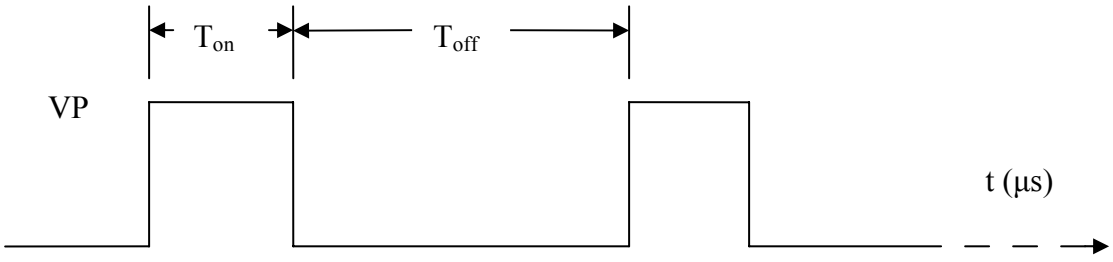

Fig.4.3 Graphical representation of sparking cycles

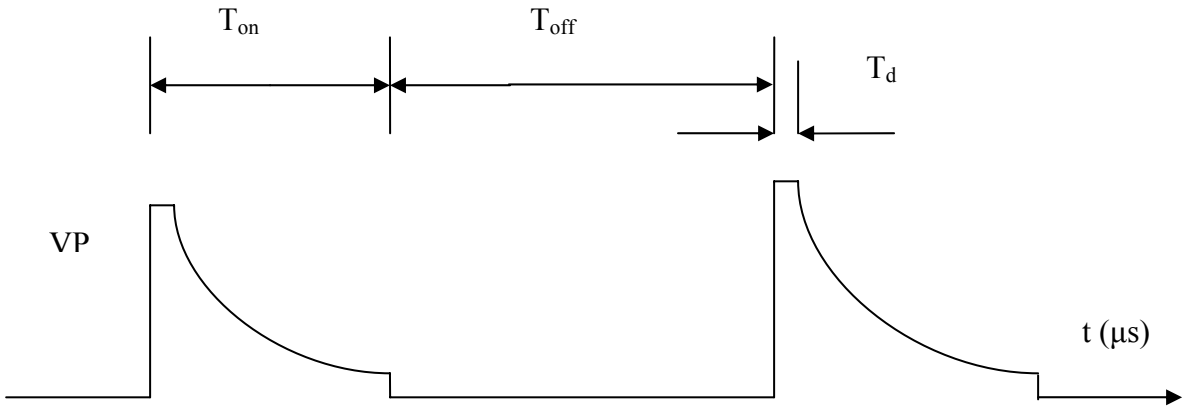

Fig.4.4 Series of electrical pulses at the inter electrode gap

T_{on}: Pulse ON time

T_{off}: Pulse OFF time

T_d: Spark Ignition Period

V_P: Open Gap Voltage

V_g: Average Gap Voltage

The work material was mounted on the T-slot table and positioned at the desired place and clamped. The electrode was clamped and its alignment was checked. The machining time was set as 5 minutes. Finally the required power switches were switched 'ON' for operating the desired discharge current values.

After each machining operation, the work piece material was taken out and weighed to find out the weight loss. From the weight loss obtained, the material removal rate was calculated for different current values. Three cases were considered with varying T_{on} conditions and machining was done for four different current values in each case. After the machining was done the change in weight of the material was calculated. From the weight change, the volume of material removed was found out and finally the Material Removal Rate was calculated.

Table 4.2 shows the EDM machining parameters for this 12 conditions set during machining.

Table 4.2 EDM machining parameters

ExptNo.	BLOCK	STEP	X	Y	Z	I_p	T_{on}	t	V_g	SEN	ASEN	TW	T↑	POL
1	S	1	0	0	-9	5	100	10	50	7	2	1.5	0.3	+ve
	E	2	0	0	-9	5	100	10	50	7	2	1.5	0.5	+ve
2	S	1	0	0	-9	15	100	10	50	7	2	1.5	0.3	+ve
	E	2	0	0	-9	15	100	10	50	7	2	1.5	0.5	+ve
3	S	1	0	0	-9	35	100	10	50	7	2	1.5	0.3	+ve
	E	2	0	0	-9	35	100	10	50	7	2	1.5	0.5	+ve
4	S	1	0	0	-9	45	100	10	50	7	2	1.5	0.3	+ve
	E	2	0	0	-9	45	100	10	50	7	2	1.5	0.5	+ve
5	S	1	0	0	-9	5	150	10	50	7	2	1.5	0.3	+ve
	E	2	0	0	-9	5	150	10	50	7	2	1.5	0.5	+ve
6	S	1	0	0	-9	15	150	10	50	7	2	1.5	0.3	+ve
	E	2	0	0	-9	15	150	10	50	7	2	1.5	0.5	+ve
7	S	1	0	0	-9	35	150	10	50	7	2	1.5	0.3	+ve
	E	2	0	0	-9	35	150	10	50	7	2	1.5	0.5	+ve
8	S	1	0	0	-9	45	150	10	50	7	2	1.5	0.3	+ve
	E	2	0	0	-9	45	150	10	50	7	2	1.5	0.5	+ve
9	S	1	0	0	-9	5	200	10	50	7	2	1.5	0.3	+ve
	E	2	0	0	-9	5	200	10	50	7	2	1.5	0.5	+ve
10	S	1	0	0	-9	15	200	10	50	7	2	1.5	0.3	+ve
	E	2	0	0	-9	15	200	10	50	7	2	1.5	0.5	+ve
11	S	1	0	0	-9	35	200	10	50	7	2	1.5	0.3	+ve
	E	2	0	0	-9	35	200	10	50	7	2	1.5	0.5	+ve
12	S	1	0	0	-9	45	200	10	50	7	2	1.5	0.3	+ve
	E	2	0	0	-9	45	200	10	50	7	2	1.5	0.5	+ve

Table 4.3 represents the description of the programming parameters and their ranges [37]. These programming parameters are present in the working area where the user is allowed to edit the program parameters.

Table 4.3 Description of the programming parameters and their ranges

Parameters	Description	Range
X	X Displacement	-999.0 to 9999.99
Y	Y Displacement	-999.0 to 9999.99
Z	Z Depth	-999.0 to 9999.99
Ip	Sparking Current	0-200 A for normal machining (depending on machine model)
Ton	Pulse ON Time	0.5-4000 μ secs
t	Duty Cycle	1 - 12
Vg	Gap Voltage	40-100
SEN	Sensitivity (Quill Speed)	1- 10
ASEN	Antiarc Sensitivity	1- 10
TW	Work Time	0.1 – 30 secs
T↑	Lift Time	0.0 to 20 secs

The experiment was conducted and the weight of material removed was checked after each operation. The results obtained are shown in Chapter-5, Table 5.2. The calculation for material removal rate was done as per the sample calculation shown in 4.1.

4.1 SAMPLE CALCULATION:

For Ton=100, the Material removal rates at 4 different current values are:

(1) Current = 5 Amperes

The initial weight of the sample = 178.430 grams

After machining, the final weight = 178.270 grams

Weight loss = 178.430 – 178.270 grams = 0.160 grams

Volume Loss = Weight loss / Density

= 0.160 / 0.0077 mm^3

= 20.779 mm^3

Material Removal Rate = Volume of the material removed /Time

= 20.779 / 5= 4.1558 mm^3/min.

The electrode and work piece material after the machining operation is shown in Fig. 4.5.

Fig.4.5 shows the electrode and work piece after the machining operation.

CHAPTER – 5

The main cause for material removal from both tool and work piece is the temperature reached at their surfaces. The material evaporates from both tool and work piece where the temperature is above the melting temperatures of the respective materials. This temperature at the surface of both the electrodes is due to the thermal energy, which is generated in the discharge channel. The first step in the prediction of thermal stresses is the analysis of temperature distribution. Thermal action of EDM process also affects the surface integrity of the machined component.

The tool and work piece material is considered as copper and EN-19 respectively during the model analysis. The temperature distribution during single discharge was calculated with energy input. After the single pulse discharge ignited, discharge channel changes from ambient liquid to plasma with channel expansion. The thermal energy generates a channel of plasma between the electrodes at temperature in the range of 8000 to 12,000 °C or as high as 20,000 °C initializing a substantial amount of heating and melting of material at the surface of each pole. This temperature obtained is the maximum temperature reached in the discharge channel and it is an indicator of the model's thermal behavior. This temperature distribution was used to calculate the volume of material removed from the work piece for different current intensities.

5.1 VOLUME OF MATERIAL REMOVED

During computation of results using FEM, the width and depth of crater in the work piece for a single spark is predicted assuming that the regions which attain a temperature above the upper limit of melting temperature (10,000ºC) are completely removed [1].

In Fig. 5.1, the temperature distribution of discharge channel at current intensity 68 amps is shown and the maximum temperature reached in the discharge channel is 17881˚C, which is also the maximum temperature reached in the work piece. Where as the maximum temperature of the tool is about 10,000˚C. Hence, the heat dissipated in the work piece is more than the tool.

Considering the crater of material removed as an ellipsoid as shown in Fig. 5.1, its radii are represented as r_1, r_2 and r_3. The radii r_1 is equal to r_2 as the volume is axisymmetric. These radii r_1 and r_3 are measured from Fig. 5.1 after multiplying with appropriate scale factor; the volume of material removed is calculated and found to be 1.853856×10^9 μm^3. For a current intensity of 68 amps, the volume of material removed was calculated as per the sample calculation.

5.2 SAMPLE CALCULATION:

The Volume of material removed for current 68 amps is given as:

Volume of ellipsoid = $4/3\ \Pi\ r_1\ r_2\ r_3$

Here r_1= 1.2 mm, r_2 = 1.2 mm, r_3 = 0.615 mm

So, Volume = 4/3 x 3.14 x 1.2x 1.2 x 0.615

= 3.7077 mm^3

Volume of material removed = ½ volume of ellipsoid

= ½ x 3.7077

=1.853856 mm^3

=1.853856×10^9 μm^3

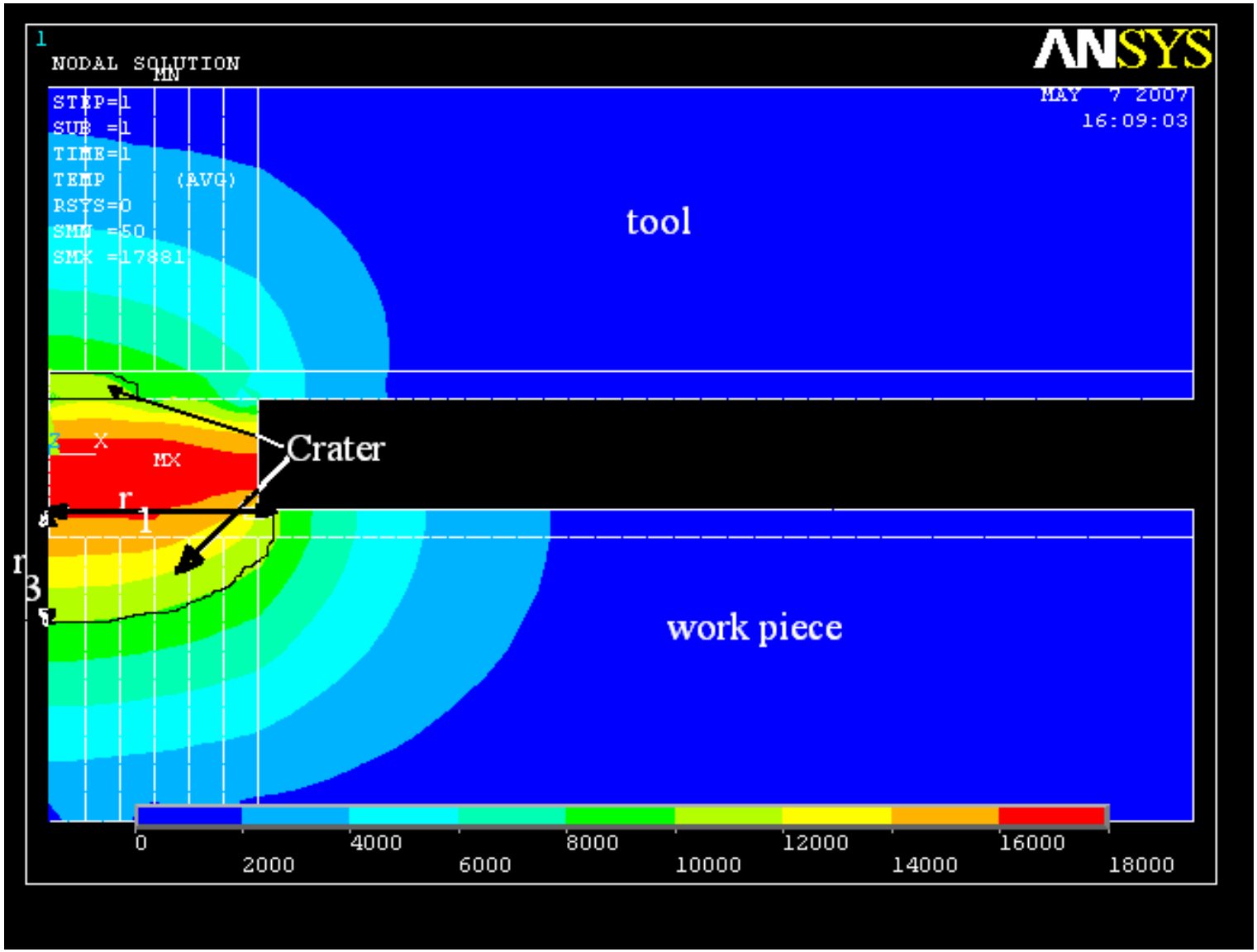

Fig. 5.1 Temperature distribution obtained for a current intensity value of 68 amps

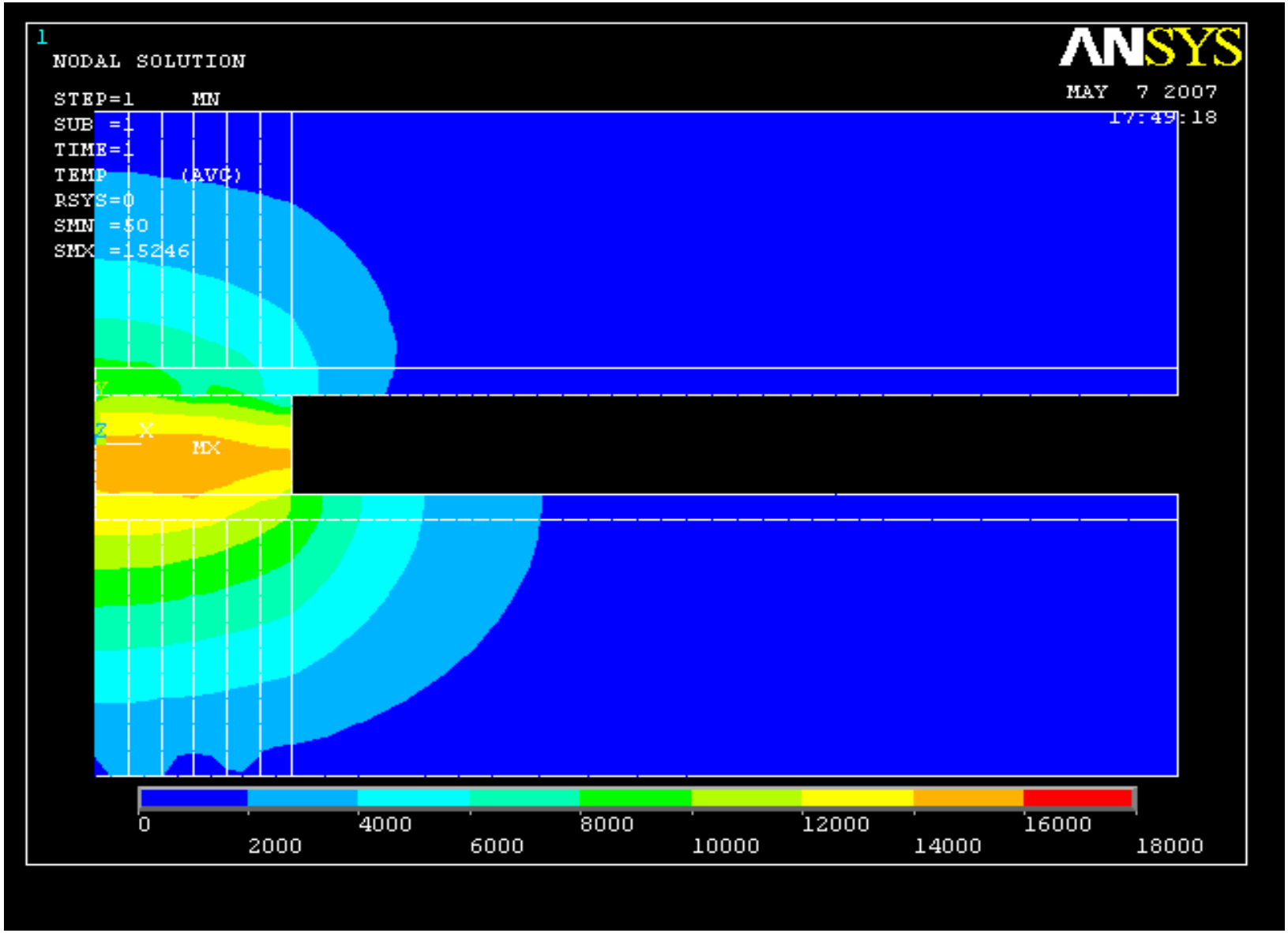

Fig. 5.2 Temperature distribution obtained for a current intensity value of 58 amps

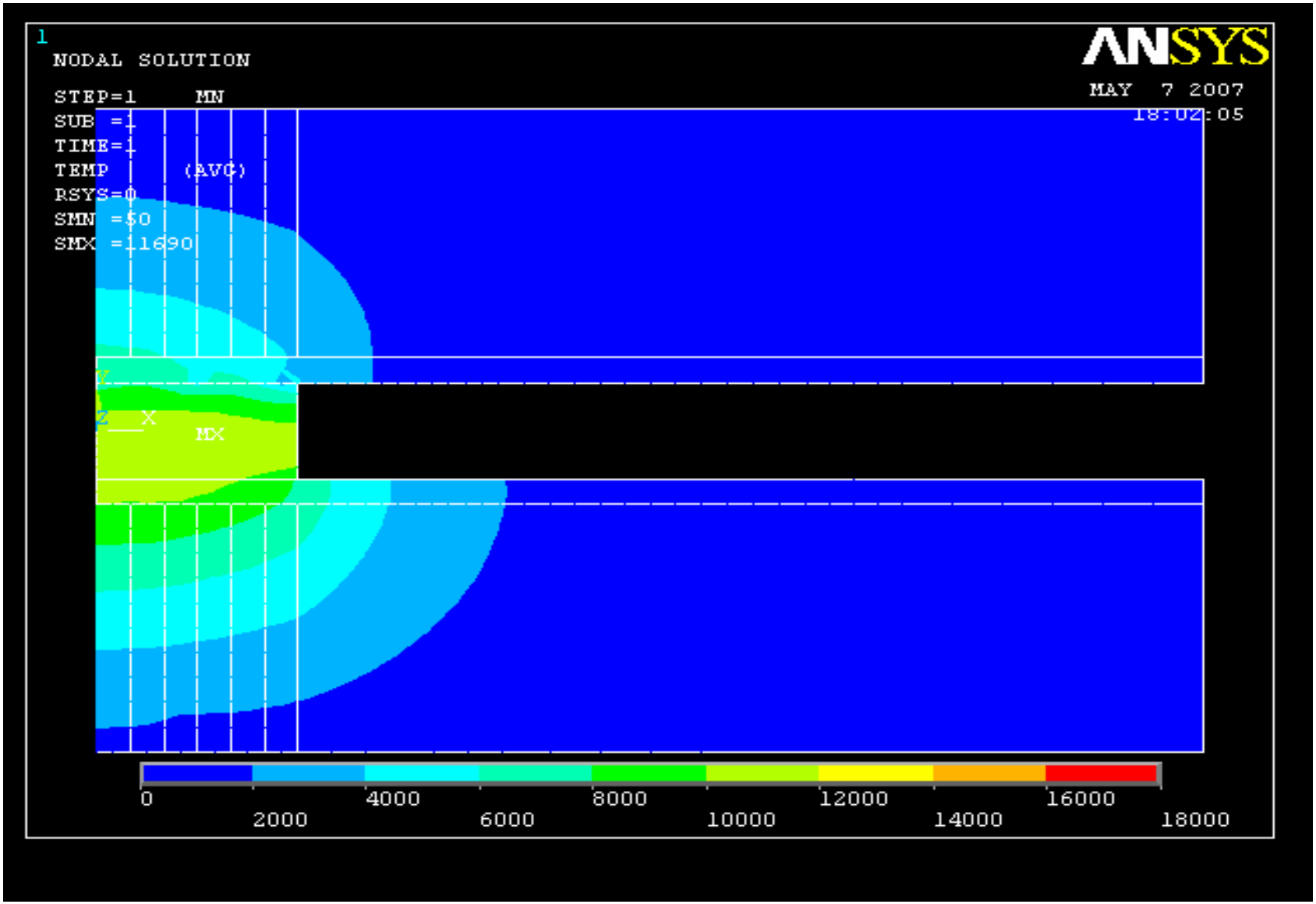

Fig. 5.3 Temperature distribution obtained for a current intensity value of 44 amp

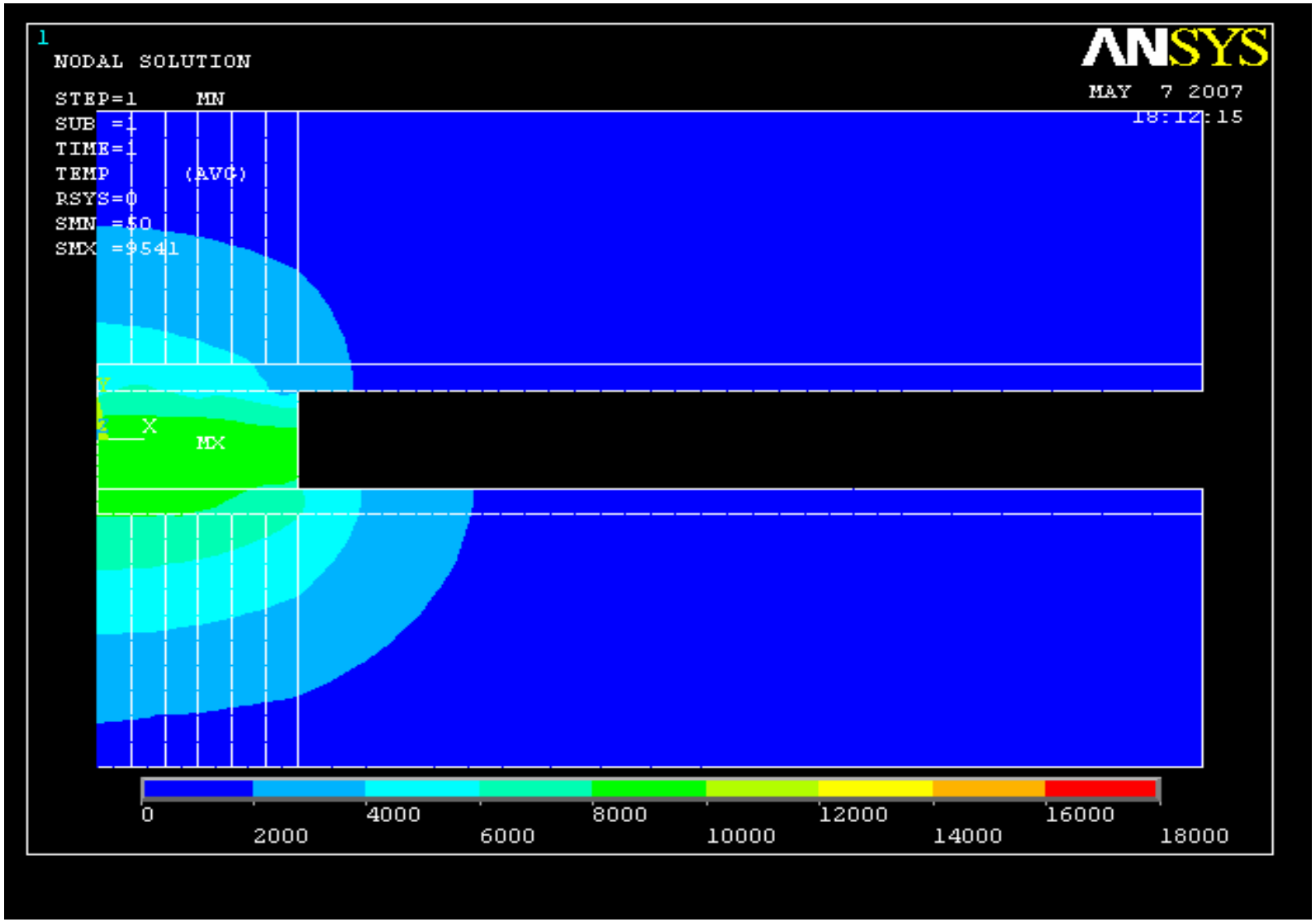

Fig. 5.4 Temperature distribution obtained for a current intensity value of 36 amps

Fig. 5.2 shows the temperature distribution at 58 amps and the maximum temperature reached in the discharge channel is 15,246ºC. The maximum temperature reached in the work piece is about 14,000ºC where as the maximum temperature of tool is about 10,000ºC.Thus, the heat dissipated in the work piece is more than the tool. With the decrease in current intensity, temperature decreases as a result of which the area subjected to more than 10,000ºC is decreasing. The volume of material removed from the work piece is 1.098748 μm^3 x 10^9 which is less than the volume of material removed for 68 amps.

For a current intensity of 44 amps, maximum temperature reached in the discharge channel is 11,690ºC as shown in Fig.5.3. The maximum temperature reached in the work piece is about 12,000ºC where as the maximum temperature reached in the tool is about 10,000ºC. Again the heat dissipated in the work piece is more than the tool. The volume of material removed in this case is 0.181366 x 10^9 μm^3.

Similarly, for a current intensity of 36 amps, the maximum temperature reached in the discharge channel is 9,541ºC which is comparatively less than the maximum temperature of discharge channel for 68 amps, 58 amps and 44 amps. With the decrease in current intensity, area subjected to a temperature of 10,000ºC is also decreasing consequently decreasing the volume of material removed which is calculated as 0.090432 x 10^9 μm^3.

The table containing the values of r_1, r_2, r_3, current intensities, volume of material removed and R_{max} is presented in Table 5.1. The radii of the crater formed r_1, r_2 and r_3 is represented by an ellipsoid. With different current intensity (I) values, the volume of material removed is shown in the table. The calculated maximum surface roughness (R_{max}) values are also shown which are the r_3 values of the ellipsoid representing the crater.

Table 5.1 Table for FEA results of r_1, r_2, r_3, current intensities, volume of material removed and R_{max}

Sl. no.	Radii of the ellipsoid representing crater formed			Current Intensity (I) (amps)	Volume of material removed (μm^3) x 10^9	R_{max} (mm)
	r_1 (mm)	r_2 (mm)	r_3 (mm)			
1	1.2	1.2	0.615	68	1.853856	0.615
2	1.08	1.08	0.45	58	1.098748	0.45
3	0.76	0.76	0.15	44	0.181366	0.15
4	0.6	0.6	0.12	36	0.090432	0.12

A graph showing the volume of material removed for different current intensities is presented in Fig. 5.5. It is clear from the plot that the volume of material removed decreases with decrease in current. From 68 amps to 44 amps, the volume of material removed decreases uniformly where as from 44 amps to 36 amps there is a little decrease in volume of removed material.

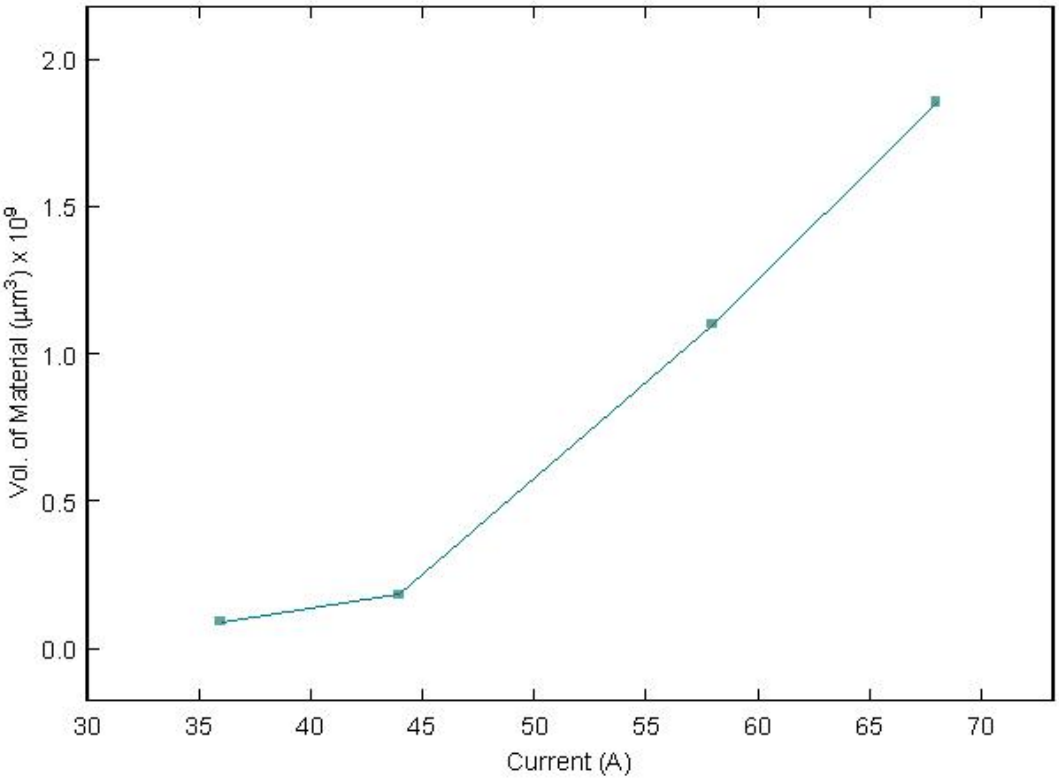

Fig. 5.5 Volume of material removed with different current intensities for FEA

5.3 MAXIMUM SURFACE ROUGHNESS (R_{MAX}):

The application of Electric Discharge Machining technique induces severe surface morphological and elemental alterations due to the high temperatures developed during machining, which vary between 10,000°C and 20,000°C. The distinctive morphology of a surface which has undergone EDM machining, is due to the enormous amount of heat generated by the discharges, which causes melting and vaporization of the material, followed by rapid cooling. The surface roughness is caused by an uneven fusing structure, globules of debris, shallow craters, pockmarks, voids and cracks. These effects become more pronounced as the pulse current and pulse-on duration increase.

In the present work, the maximum work piece (cathode) surface roughness (R_{max}) is calculated for different current intensity values.

For a current intensity value of 68 amps, the temperature reached by the discharge channel is 17,881°C as shown in Fig. 5.1. The maximum surface roughness (R_{max}) value obtained for the work piece is found to be 0.615mm. As the temperature reached by the discharge channel is more, the depth of crater is also more as a result of which R_{max} is more. The depth of crater depends on the average power intensity of spark.

The R_{max} value obtained for the work piece is found to be 0.45mm for a current intensity of 58 amps. The maximum temperature reached in the discharge channel is 15,690°C which is less in comparison to 68 amps which lowers the depth of crater and R_{max} decreases subsequently.

For a current intensity value of 44 amps, the R_{max} value obtained for the work piece is be 0.15mm which is less as compared to that for a current intensity of 68 amps and 58 amps depending upon the maximum temperature reached in the discharge channel and work piece.

The R_{max} value obtained for the work piece is found to be 0.12mm for a current intensity value of 36 amps. As the temperature reached by the discharge channel is less compared to 68 amps, 58 amps and 44 amps, the depth of crater is also less as a result of which R_{max} is less.

A graph showing the respective R_{max} values with the corresponding current intensities is presented in Fig. 5.6. Better surface finish is obtained with less current. So, for finishing cut the current should be less as possible.

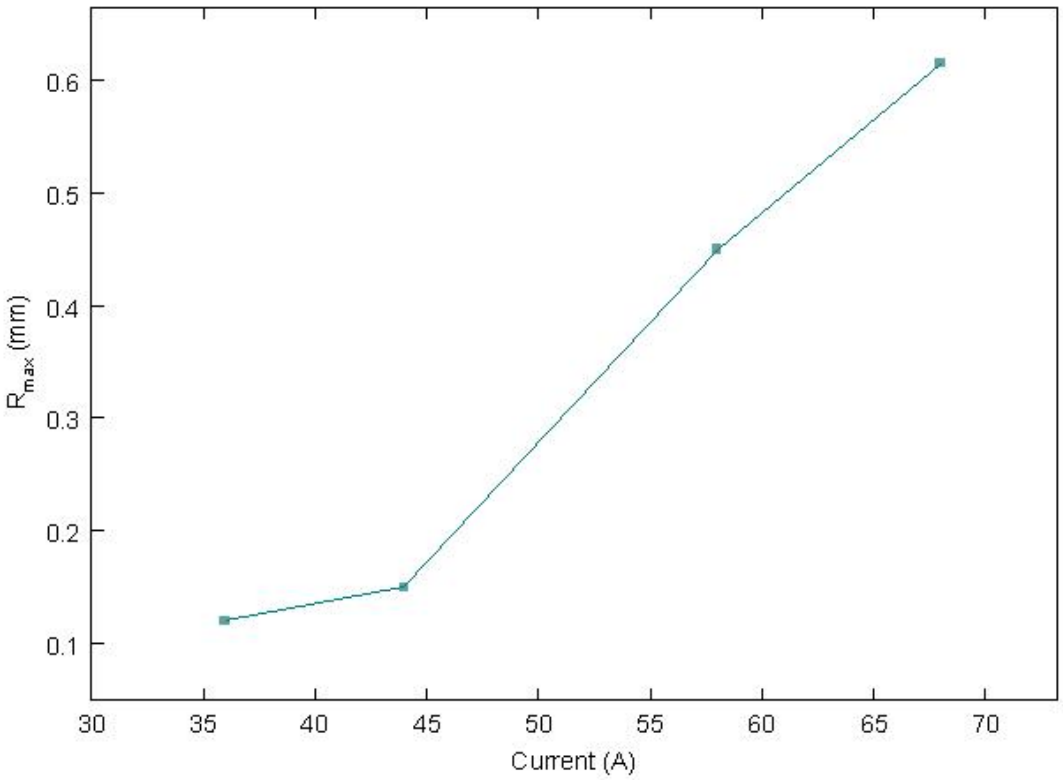

Fig. 5.6 R_{max} values with various current intensities for FEA

5.4 EXPERIMENTAL RESULTS:

The material removal rate found in the experiment conducted with varying T_{on} and current values are shown in Table 5.2. The difference in weights, volume of material removed and material removal rates are also presented in the table.

Table 5.2 Material removal rate found in the experiment conducted with varying T_{on} and current values

Expt.No.	I_p (Amps)	Ton	Machining Time(min)	Initial Weight (grams)	Final Weight (grams)	Difference in Weight (grams)	Volume of material removed (mm^3)	MRR (mm^3/min)
1	5	100	5	178.43	178.27	0.16	20.78	4.16
2	45	100	5	178.27	174.62	3.65	474.03	94.81
3	35	100	5	174.62	171.42	3.20	415.58	83.12
4	15	100	5	171.42	169.97	1.45	188.31	37.66
5	5	150	5	170.01	169.81	0.20	25.97	5.19
6	15	150	5	169.81	168.01	1.80	233.77	46.75
7	35	150	5	168.01	164.18	3.83	497.40	99.48
8	45	150	5	164.18	159.56	4.62	600.00	120.00
9	5	200	5	159.56	159.34	0.22	28.57	5.71
10	15	200	5	159.34	157.18	2.20	285.71	57.14
11	35	200	5	157.18	153.10	4.63	601.30	120.26
12	45	200	5	153.10	148.61	5.62	729.87	145.97

A graph showing the material removal rates with varying current conditions and different T_{on} values is presented in Fig. 5.7. It indicates that for T_{on} =100, with increase in current the material removal rate increases. The volume of material removed is increasing as the current is increasing and hence the Material Removal Rate is also increasing for T_{on} = 150 and 200.

The material removal rate increases with T_{on} for same current which is obvious. As spark time increases with T_{on}, more energy is being released in the discharge channel and consequently more is the material removal rate.

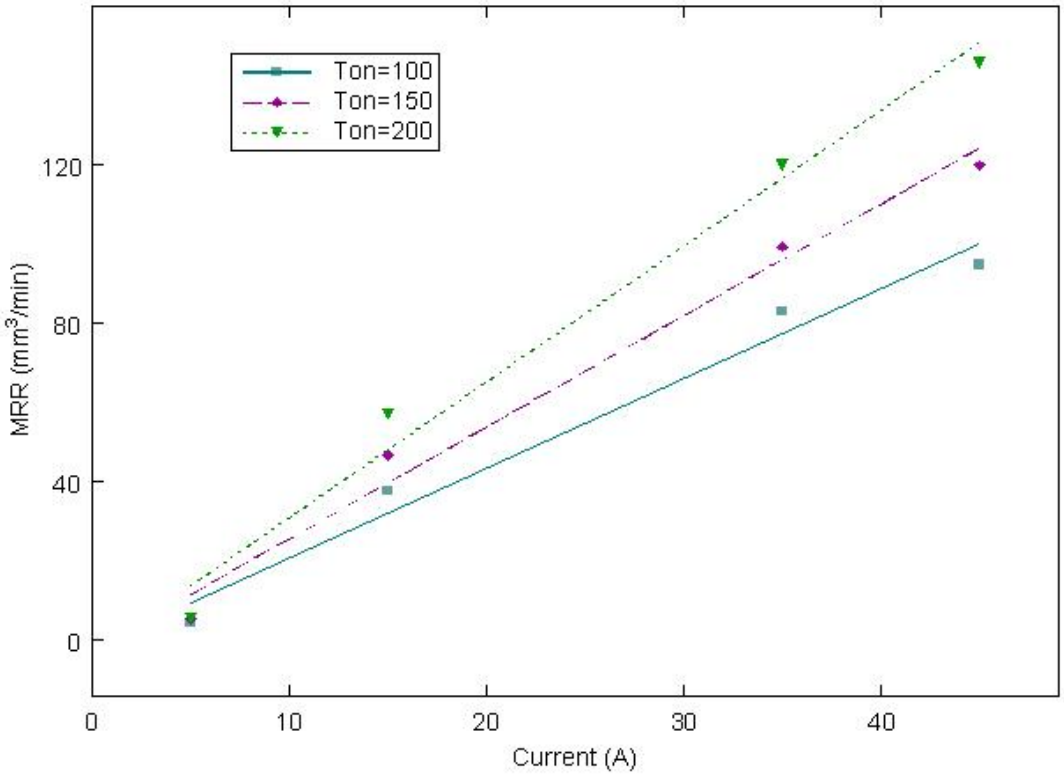

Fig. 5.7 Material Removal rates with varying current conditions for Experiment.

CHAPTER – 6

6.1 CONCLUSION

In the present work, the Joule heating factor was used to model the EDM process and predict the maximum temperature reached in the discharge channel. From the temperature distribution the volume of material removed from the work piece and R_{max} was estimated. Experiments were conducted with different pulse on-time (T_{on}) and current values and the material removal rate was calculated. The Most important conclusions of the work are:

1. With the new FEA model for the EDM process, it is possible to estimate the material removed from the work piece, the surface roughness and the maximum temperature reached in the discharge channel. The maximum temperature in the discharge channel is an indicator of the model's thermal behaviour.

2. Material removal rate increases with the increase in current.

3. Maximum surface roughness (R_{max}) increases with the increase in current.

4. From the experiments conducted, the volume of material removed and material removal rate is calculated and its trend in variation with current is in agreement with FEA results.

5. The 2D axisymmetric finite element analysis can be solved easily and computation takes few seconds only.

6.2 SCOPE FOR FUTURE WORK:

Single discharge process is completed by thermal and electric analysis. Successive multi discharge is superposition of successive single discharge. For multi discharge process simulation, the next ignition point should be found after single discharge process. To find next ignition point, electric field analysis has to be conducted. Electric field strength between electrode and work piece is the function of surface configuration, dielectric constant of dielectric fluid, discharge gap and applied voltage. In electric field analysis, if the electric strength is higher than dielectric breakdown strength, this point is the next ignition position. From the next ignition position, the next single discharge simulation could be conducted. From the repetition of thermal-electric field analysis, successive discharge process could be simulated.

The model is an integrated one, so it can be allowed to submit simultaneously cathode and anode in the same problem and same work conditions and further the material removed from anode can also be found out. This will also lead to calculation of Material Removal Efficiency given as the ratio of material removed per pulse to the volume melted per pulse.

REFERENCES

1. Ho.K.H and Newman.S.T., "State of the art electrical discharge machining (EDM)" International Journal of Machine Tools & Manufacture, Volume 43, (2003): p. 1287–1300.
2. Narasimhan Jayakumar, Yu Zuyuan and P. Rajurkar Kamlakar, "Tool wear compensation and path generation in micro and macro EDM" Transactions of NAMRI/SME, Volume 32, (2004): p.1-8.
3. Das Shuvra, Mathias Klotz and Klocke.F, "EDM simulation: finite element-based calculation of deformation, microstructure and residual stresses" Journal of Materials Processing Technology, Volume 142, (2003):p.434-451.
4. Abbas Mohd Norliana, Solomon.G.Darius and Bahari Fuad Md., "A review on current research trends in electrical discharge machining (EDM), International Journal of Machine Tools & Manufacture, Volume 47, (2007):p.1214-1228.
5. Schumacher M.Bernd, "After 60 years of EDM the discharge process remains still disputed" Journal of Materials Processing Technology, Volume 149,(2004):p.376-381.
6. Benedict.F.Gray, "Nontraditional Manufacturing Processes" Marcel Dekker,(1987):p.209
7. Yan.B.H, Lin.Y.C and Huang.F.Y, "Surface modification of Al–Zn–Mg alloy by combined electrical discharge machining with ball burnish machining" International Journal of Machine Tools & Manufacture, Volume 42, (2002):p.925-934.
8. Puertas.I and Luis C.J, "A study on the machining parameters optimisation of electrical discharge machining" Journal of Materials Processing Technology, Volume 143- 144, (2003):p. 521–526.
9. Lee Hiong Soo and Li Xiaoping, "Study of the surface integrity of the machined work piece in the EDM of tungsten carbide" Journal of Materials Processing Technology, Volume 139,(2003):p.315-321.

10. Guu Y.H., Ti-Kuang Hou Max, " Effect of machining parameters on surface texturesin EDM of Fe- Mn -Al alloy" Materials Science and Engineering , Volume:35(2007):p.237-245.

11. DiBitonto.D.D., Eubank P.T., Patel M.R. and Barrufet.M.A, "Theoretical models of the electrical discharge machining process-I: a simple cathode erosion model" Journal of Applied Physics, Volume 66, (1989):p.4095–4103.

12. Patel.M.R., Barrufet.M.A., Eubank.P.T. and DiBitonto.D.D, "Theoretical models of the electrical discharge machining process-II: the anode erosion model" Journal of Applied Physics, Volume 66, (1989):p. 4104–4111.

13. Madhu.P, Jain.V.K.and Sundararajan.T, "Analysis of EDM process: A Finite Element Approach", Computers in Engineering ASME, (1991), Volume 2:p.121-127.

14. Eubank.P.T, Patel.M.R., Barrufet.M.A. and Bozkurt.B, "Theoretical models of the electrical discharge machining process-III: the variable mass, cylindrical plasma model", Journal of Applied Physics, Volume 73, (1993):p. 7900–7909.

15. Basak Indrajit and Ghosh Amitabha, "Mechanism of material removal in electro chemical discharge machining: a theoretical model and experimental verification" Journal of Materials Processing Technology, Volume 71, (1997):p.350-359.

16. Rebelo J.C., Dias A. Morao, Mesquita Ruy, Paulo Vassalo and Mario Santos, "An experimental study on electro-discharge machining and polishing of high strength copper-beryllium alloys" Journal of Materials Processing Technology, Volume 108, (2000):p.389-397.

17. Che Haron .C.H, Md. Deros .B, Ginting.A. and Fauziah.M, "Investigation on the influence of machining parameters when machining tool steel using EDM" Journal of Materials Processing Technology, Volume 116, (2001):p.84-87.

18. Kulkarni A., Sharan R. and Lal G.K., "An experimental study of discharge mechanism in electrochemical discharge machining" International Journal of Machine Tools & Manufacture, Volume 42, (2002):p.1121-1127.

19. Yadav Vinod, Jain Vijay K.and Dixit Prakash.M., "Thermal stresses due to electrical discharge machining" International Journal of Machine Tools & Manufacture, Volume 42, (2002):p.877-888.

20. Wang Kesheng, Gelgele Hirpa L., Wang Yi , Yuan Qingfeng , Fang Minglung, "A hybrid intelligent method for modelling the EDM process" International Journal of Machine Tools & Manufacture, Volume 43, (2003):p.995-999.

21. Lee H.T. and Tai T.Y., "Relationship between EDM parameters and surface crack formation" Journal of Materials Processing Technology, Volume 142, (2003):p.676-683.

22. Valentincic Josko and Junkar Mihael, "On-line selection of rough machining parameters" Journal of Materials Processing Technology, Volume 149, (2004):p.256-262.

23. Lauwers B. , Kruth J.P. , Liu W. , Eeraerts W. , Schacht B. and Bleys P., "Investigation of material removal mechanisms in EDM of composite ceramic materials" Journal of Materials Processing Technology, Volume 149, (2004):p.347-352.

24. Singh Shankar, Maheshwari S. and Pandey P.C., "Some investigations into the electric discharge machining of hardened tool steel using different electrode materials" Journal of Materials Processing Technology, Volume 149, (2004):p.272-277.

25. Sharakhovsky Leonid I. , Marotta Aruy and Essiptchouk Alexei M., "Model of work piece erosion for electrical discharge machining process" Applied Surface Science, Volume 253, (2006): p.797–804.

26. Salah Nizar Ben, Ghanem Farhat and Atig Kaıs Ben, "Numerical study of thermal aspects of electric discharge machining process" International Journal of Machine Tools & Manufacture, Volume 46, (2006):p.908-911.

27. Bhondwe K.L., Yadava Vinod, Kathiresan G., "Finite element prediction of material removal rate due to electro-chemical spark machining" International Journal of Machine Tools & Manufacture, Volume 46, (2006):p.1699-1706.

28. Marafona J. and Chousal J.A.G., "A finite element model of EDM based on the Joule effect" International Journal of Machine Tools & Manufacture, Volume 46, (2006):p.595-602.

29. Allen Philip, Chen Xiaolin, "Process simulation of micro electro-discharge machining on molybdenum" Journal of Materials Processing Technology, Volume 186, (2007):p.346-355.

30. Erden A., "Effect of materials on the mechanism of electric discharge machining (EDM)" Transactions ASME, Journal of Engineering Materials and Technology, Volume 108, (1983): p.247–251.

31. Pandey P.C.and Jilani S.T., "Plasma channel growth and the resolidified layer in EDM" Precision Engineering, Volume 8 (2), (1986):p. 104–110.

32. Ikai T.and Hashigushi K., "Heat input for crater formation in EDM" Proceedings of International Symposium for Electro Machining-I, Lausanne, Switzerland, April (1995):p. 163–170.

33. ANSYS coupled field analysis guide. Release 10 documents.

34. Rajan.T.V, Sharma.P.C and Sharma Ashok, Heat treatment principles and techniques, Prentice hall of India Pvt. Ltd., New Delhi,(2001):p.253-262.

35. ASM metals Handbook, Volume-1, (1978):p.124

36. Singh Vajendra, Physical Metallurgy, standard publishers distributors, New Delhi (2004):p.605-640.

37. Manual of Electronica for EDM.